R. & M. No. 3140
(20,252)
A.R.C. Technical Report

MINISTRY OF AVIATION

AERONAUTICAL RESEARCH COUNCIL
REPORTS AND MEMORANDA

The Centre-Line Mach-Number Distributions and Auxiliary-Suction Requirements for the A.R.A. 9-ft x 8-ft Transonic Wind Tunnel

By A. B. HAINES, B.Sc., and J. C. M. JONES, B.Sc.(Eng.)

LONDON: HER MAJESTY'S STATIONERY OFFICE
1960
PRICE 17*s.* 6*d.* NET

The Centre-Line Mach-Number Distributions and Auxiliary-Suction Requirements for the A.R.A. 9-ft x 8-ft Transonic Wind Tunnel

By A. B. Haines, B.Sc., and J. C. M. Jones, B.Sc.(Eng.)

*Reports and Memoranda, No. 3140**

April, 1958

Summary. Measurements of the centre-line Mach-number distributions have been made in the Aircraft Research Association 9-ft × 8-ft Transonic Wind Tunnel over the range of Mach numbers from 0·6 to 1·4. At subsonic speeds up to $M = 1 \cdot 00$, a standard of flow uniformity corresponding to $\Delta M = \pm\ 0 \cdot 002$ was achieved over a test-section length of about 6 ft. Between $M = 1 \cdot 00$ and $M = 1 \cdot 10$, when the supersonic stream is generated merely by auxiliary suction through the perforated walls, significant improvements in flow uniformity were achieved by modifications to the open area distributions at the upstream end of the side perforated walls and as a result, $\Delta M \leqslant \pm\ 0 \cdot 005$ up to about $M = 1 \cdot 10$. At $M = 1 \cdot 10$, the uniform flow is generated within a distance of about 0·4 × tunnel height from the start of the perforated plate.

Almost the same standard of flow uniformity is achieved with the $M = 1 \cdot 15$ and $M = 1 \cdot 20$ nozzles by running at the optimum Mach numbers and with the best wall settings for these nozzles. At higher Mach numbers, however, the quality of the flow deteriorates somewhat, the values of ΔM being $\pm\ 0 \cdot 010$ for $M = 1 \cdot 25$, $\pm\ 0 \cdot 012$ for $M = 1 \cdot 35$ and $\pm\ 0 \cdot 016$ for $M = 1 \cdot 4$. This deterioration is largely due to disturbances originating from near the saw-tooth junction of the nozzle and perforated plate on the floor.

Apart from these disturbances, ΔM is within $\pm\ 0 \cdot 007$ throughout the Mach number range, *i.e.*, up to $M = 1 \cdot 4$. All these quoted values for ΔM are probably conservative because they include measurement errors, etc.

To achieve these standards, the side perforated walls should be either parallel or converged by not more than 6 minutes; use of more convergence results in a poorer standard of flow uniformity for all Mach numbers greater than 1·06.

The distributions presented dictate that the model nose should not be placed ahead of 0·4 × tunnel height downstream of the start of the perforated side wall and the model tail should if possible be ahead of 0·35 × tunnel height upstream of the end of the perforated plate. This leaves about 6 ft available as a maximum model length.

A Mach number of 1·4 at a stagnation pressure of 1 Atm and with the tunnel empty is achieved with a total power of 440 h.p./sq ft working-section area and with a flow removal from the plenum chamber of only about 1·8 per cent of the mass flow through the throat. There is sufficient fan pressure ratio and auxiliary-suction capacity in hand to maintain this Mach number with a complete model at a lift coefficient of 0·75 present in the working-section.

1. *Introduction.* The A.R.A. 9-ft × 8-ft Transonic Wind Tunnel has a working-section with four perforated walls, an auxiliary suction plant for air removal from the plenum chamber surrounding the working-section, and also a flexible nozzle which is used to generate the supersonic stream for Mach numbers of 1·14 and above. This report is concerned with presenting and discussing the

* A.R.A. Report No. 2, received 17th June, 1958.

centre-line Mach-number distributions obtained during the calibration. It shows how these are affected by changes in suction quantity, wall geometry and nozzle setting and also how, particularly at low supersonic Mach numbers, they have been improved by modifications to the distribution of wall porosity along the length of the working-section.

Other aspects of the calibration, *e.g.*, the Mach-number distributions at positions off the centre-line, the distributions of flow inclination and total-head pressure and also results indicating the wave-reflection properties of the working-section walls will be discussed in later reports. The wave-reflection properties are, of course, of vital importance, particularly between about $M = 0 \cdot 95$ and $M = 1 \cdot 20$, the range in which reflected waves, if they exist, might strike the model under test. Hence, in this range, uniformity of centre-line Mach-number distribution is not the only criterion on which to judge what is the optimum wall setting to choose for a given Mach number. It may be that the optimum setting is not the one that gives the most uniform distribution. For this reason, the present report gives not only the best distributions but also those obtained over quite a wide range of perforated wall and nozzle settings.

This need to meet different, possibly conflicting requirements, also affects what is the best longitudinal distribution of wall porosity. The modifications described in this report were all designed to improve the standard of the distributions for the case when the walls are parallel. If it is found later, for example, that for the sake of better alleviation of reflected waves, the walls should be converged, further modifications to the porosity leading to changes in the flow distributions as given here might then be desirable. The detailed analysis of tests made to investigate the reflected wave characteristics has, however, not yet been completed.

The centre-line Mach-number distributions are discussed in turn for three ranges of Mach number:

(1) Subsonic speeds up to near $M = 1 \cdot 0$: in this range, no auxiliary suction is required and the only variables are fan pressure ratio, convergence of working-section walls, and the setting of the walls opposite the model support strut: the last two variables determine the amount of diffuser-suction effect.

(2) Between $M = 1 \cdot 0$ and about $M = 1 \cdot 12$: in this range, the supersonic stream is generated by auxiliary suction through the working-section walls and no changes are made to the shape of the flexible nozzle.

(3) $M = 1 \cdot 14$ and above: in this range, the supersonic stream is basically generated by the flexible nozzle. The auxiliary suction and wall angle are adjusted to provide minor variations in Mach number as compared with the Mach number at the end of the nozzle, to maintain as uniform a flow as possible throughout the length of the working-section and to provide at least some measure of alleviation of reflected waves.

The report also contains some limited data regarding the power and auxiliary-suction requirements of the tunnel.

2. *Description and Operation of Tunnel.* 2.1. *Description of the Tunnel.* Fig. 1 shows the essential features of the tunnel circuit and Figs. 2a and 2b are a more detailed presentation of the region enclosed by the pressure shell or plenum chamber. This region can be thought of in three parts: the flexible nozzle, the working-section and third, the section surrounding the model support strut.

The flexible nozzle upstream of the working-section is intended as a means of flow generation to be supplemented by auxiliary suction through the perforated walls. As may be seen from Fig. 2a, the nozzle shapes are achieved on the horizontal walls, the vertical walls remaining parallel. The various nozzle shapes are fixed by means of sets of stepped cams giving the following design Mach numbers at the exit of the nozzles: 1·0, 1·15, 1·20 and up to 1·40 at intervals of 0·05 and, in addition, 1·5 and 1·6. The latter two nozzle settings are to allow for possible future development of the tunnel. The nozzle ordinates are given in the Appendix and the actual shapes achieved agreed with the design ordinates within limits of $\pm$ 0·005 in. As will be seen later, the Mach numbers attained at the end of the nozzles are in general within about 0·01 of the design values.

The working-section itself is defined as the length enclosed by the perforated plates on the vertical side walls. The longitudinal datum for all the figures in this report is taken as the leading edge of these walls. The perforated walls on the top and bottom sides start 20 in. downstream of this datum and the perforated plate on all four walls ends at a point 146 in. downstream of the datum. The full length of perforated section is therefore only 1·44 $\times$ (mean of the working-section height and width), which is very much less than in many other transonic tunnels*.

The lower horizontal perforated wall is nominally horizontal while on the upper wall, allowance is made for the growth of boundary-layer thickness, estimated as 0·001 per in. per wall. The convergence of the side perforated walls can be varied between the limits of 1·2 deg and $-$ 1·8 deg by rotating the walls about a vertical hinge 24 in. upstream of their leading edges (Fig. 2b). The corresponding range of movement of the trailing edge is 3 in. and $4\frac{1}{2}$ in. out from the nominal parallel position. In view of some of the results presented later, it should be noted particularly that when the walls are converged or diverged, there is a change in slope on the side walls of the tunnel at a point which is within the nozzle section.

For half-model tests, part of the lower horizontal perforated wall is replaced by a solid wall to serve as a reflection plate.

The perforated plate is 0·187 in. thick and the holes are of 0·5 in. diameter and are drilled at 1 in. pitch in longitudinal rows 0·866 in. apart; the rows of holes in the lateral direction are inclined at 60 deg to the wind direction. The basic open-area ratio is 22·5 per cent but over the upstream 50 in. of the working-section, the open-area ratio is graded between zero and this final basic value in a nominally linear manner. This grading was effected by long triangular, blanking plates ('fingers') placed on the plenum-chamber side of the perforated walls. Owing to the finite hole size and spacing, the actual open-area ratio distribution over the region of graded porosity was by no means linear as can be seen from Fig. 3a (*i.e.*, original porosity). This grading was introduced on the basis of preliminary tests in a model tunnel which had shown that without it, over-expansion of the flow occurred.

In an attempt to avoid discontinuities in the flow originating from the joint between the solid nozzle and the perforated walls, a 'saw-tooth' type of joint has been adopted with a tooth apex angle of 53 deg. It was hoped that this would give effectively a 'subsonic' discontinuity at a supersonic stream speed; the success of this device is discussed later in the report.

The walls enclosing the region between the trailing edge of the working-section and the downstream end of the pressure shell (*i.e.*, between 146 in. and 297 in., downstream of the datum), are fixed on the floor and ceiling while the vertical walls have two possible movements. They can be

---

* The decision to have a relatively short length of working-section was taken for three main reasons: reduction of structural costs, lower auxiliary-suction requirements and finally, because in general the supersonic Mach numbers are generated by the flexible nozzle.

rotated about their trailing edge and also the upstream portion can be moved about a vertical hinge at approximately the mid-point of the wall (Fig. 2b). The first of these movements is possible while the tunnel is running but the second is merely adjustable. These vertical walls are referred to as the 'bent walls'. Moving them out relative to the tunnel centre-line produces a gap between the trailing edge of the porous plate and the leading edge of the bent wall so that the upstream portion of the bent wall then functions as a diffuser-suction flap, the details of which are shown on Fig. 2b. The bent-wall shape and range of adjustment were based on previous model wind-tunnel tests. The shape and position are completely defined by the angle between the upstream and downstream portions and by the distance of the leading edge from the tunnel centre-line. Nearly all the results quoted in this report apply to the case when the angle between the upstream and downstream halves is 173·5 deg and this can be assumed unless otherwise stated.

Movement of the bent wall out relative to the tunnel centre-line also relieves choking opposite the support strut which is situated in this region. The longitudinal position of the strut is adjustable over a range of about 17 in. For these tests, the strut was in its standard 'central' position for which its leading edge was at station 172·5 in. and its trailing edge at 285·5 in. Subsequent to the calibration as described in this report, the strut has been moved to its most rearward position, 8 in. further back. This point has to be remembered when considering several of the problems discussed later, *e.g.*, the position of the fall-off in Mach number at the rear of the working-section, etc.

2.2. *Operation of the Tunnel.* The primary variables controlling the general level of Mach number in the working-section are:

(*a*) Fan pressure ratio

(*b*) Auxiliary-suction quantity

(*c*) Nozzle setting

(*d*) Perforated-wall convergence.

The two-stage fan is driven by the 25,000 h.p. a.c. motor (based on 2 hours rating) on a common shaft with a 1,500 h.p. d.c. motor, the latter being part of the servo loop controlling the a.c. motor current and hence power output. At low powers, the pressure ratio is controlled by the fan rotational speed until the maximum r.p.m. of 485 is attained. Further increases of pressure ratio are then achieved by deflecting flaps on the pre-rotation vanes just upstream of the first stage and between the first and second stages of the fan.

The overall auxiliary-suction quantity (variable (*b*)) exerts some control over the working-section Mach number by removing some or all of the boundary layer on the perforated wall, and by causing an effective expansion of the working-section flow. The air so removed is re-energised by a compressor with a design pressure ratio of 3·2:1 and re-injected into the tunnel at the upstream end of the main subsonic diffuser. The auxiliary suction therefore also contributes indirectly to the overall tunnel pressure ratio by re-energising the sluggish boundary layer on the tunnel walls, by thinning the working-section boundary layer upstream of the supersonic diffuser and hence reducing losses in that region and finally by functioning as an induction pump at the point of re-injection into the main subsonic diffuser.

The auxiliary-suction compressor is driven by a 13,750 h.p. synchronous motor. Indeed, for normal operation, the compressor is run at a single point on its design r.p.m. characteristic, *i.e.*, it is run at a constant overall pressure ratio, mass flow and power. These are chosen to be sufficient to cope with the maximum mass flow likely to be required. The quantity actually being sucked from the plenum chamber is controlled by operating valves in the suction side of the circuit while the servo-operated valve in a by-pass circuit maintains the compressor mass flow and pressure ratio constant. The compressor outlet pressure is approximately atmospheric, and is therefore slightly higher than the pressure at the point of re-injection.

3. *Measurements and Accuracy.* 3.1. *Plenum-Chamber Pressure.* The pressure in the plenum chamber is, in general, approximately equal to the general level of static pressure in the working-section and is therefore a convenient reference pressure*. The question whether this relation still applies when a model is present in the working-section is outside the scope of this report. The Mach number derived from the plenum pressure and the tunnel stagnation pressure is therefore used to define the Mach number at which the tunnel is run.

3.2. *Centre-Line Static Pressure.* The centre-line static pressure was measured on a long tube, the upstream end of which was held near the end of the contraction by bracing wires from the walls. The downstream end fitted in the normal sting fitting in the model support strut. The bracing wires were tightened in such a way to counteract the sag of the tube due to its own weight. By this means, the inclination of the tube was kept within 10 minutes of the horizontal in the region of the working-section.

The diameter of the tube was $4\frac{5}{8}$ in. Two diametrically opposite rows of static holes were drilled in the surface of the tube, the holes being in the vertical plane of symmetry when the tube was in position. Both rows of holes were at 2·5 in. pitch, the upper row extending from 12·6 in. upstream of datum to 161·1 in. downstream of datum and the lower row from 36·1 in. to 116·1 in. downstream of datum. It was possible to rotate the tube through 180 deg and hence to obtain an indication of its instrument errors: this was in fact done during the calibration and the results are discussed in Section 3.6.

The static pressures were transmitted internally to the downstream end of the tube from where they were connected to multitube reservoir manometers *via* a coupling flange on the pressure shell.

3.3. *Static Pressures on the Tunnel Walls.* All the working-section walls, the downstream end of the flow-generating nozzle, the bent walls and the side walls of the main subsonic diffuser were fitted with static holes on their centre-lines at normally 2·5 in. intervals. A few static tappings were also provided upstream and downstream of the fan and cooler and at other points of interest.

3.4. *Tunnel Stagnation Pressure.* For the results presented in this report, the tunnel stagnation pressure was assumed to be equal to the static pressure in the settling length upstream of the contraction. This assumption was later justified by measurements of the total-head pressure in the working-section.

3.5. *Auxiliary-Suction Mass Flow.* The auxiliary-suction mass flow was determined by subtracting the flow through the by-pass circuit from the overall compressor mass flow. Both these quantities were determined by a calibration of the relevant parts of the compressor circuit. The

---

* This is discussed later (*see* also Fig. 25).

by-pass mass flow is uniquely determined by the angle of the by-pass valve and the outlet pressure from the compressor while the compressor mass flow was obtained from the pressure-ratio mass-flow characteristic.

3.6. *Accuracy of Measurements.* All pressures were measured on multitube manometers. Some of the static pressures from both the centre-line static tube and the tunnel walls in the region of the working-section were measured as differentials from plenum-chamber pressure, using alcohol as the fluid in the manometer. For the other pressures, mercury was used with the tunnel stagnation pressure as the reference. All the manometers were photographed during the tests and the readings required for immediate assessment were also read visually.

Maximum possible errors based on a reading accuracy of better than $\pm$ 0·05 in. of mercury are given as a function of Mach number in the following Table:

Mach number . .	0·8	0·9	1·0	1·1	1·2	1·3	1·4
Mach-number error .	0·0026	0·0026	0·0027	0·0029	0·0031	0·0034	0·0038

The above values apply when the manometer fluid was mercury; the corresponding errors for alcohol are quite negligible. In quoting Mach-number variations over the model position the readings on the alcohol manometers have normally been used.

It is impossible to evaluate the precise instrument errors at a given Mach number for individual pressure tappings on the centre-line static tube, either by rotating the tube through 180 deg or by moving it longitudinally by, say, the distance between successive tappings. In both cases, the difference between the errors at two tappings can be found but not the absolute values of either. Nevertheless, rotation of the tube through 180 deg should give a strong indication of the order of the tube errors and it should be obvious as to which is a faulty reading. Tests were therefore made with the tube in its 'normal' and 'inverted' positions. The results showed that, on the whole, the instrument errors were probably small, *i.e.*, about $\pm$ 0·001 in Mach number, except a few of the tappings which were evidently in error by up to $\pm$ 0·005 in M. It should perhaps be added that the condition of the tube was not necessarily the same throughout all the tests. The tube was removed and replaced twice, thus entailing handling, greasing, etc., so that the one error check carried out by rotating the tube is really only applicable to the results obtained near the end of the calibration. The policy followed, however, in analysing the results has been to ignore points that appear to be in error at all Mach numbers but nevertheless to continue to plot these points in all the distributions presented graphically other than the final distributions. This means that some of the small irregularities apparent in the distributions as presented can be ascribed to tube errors.

4. *Results with Diffuser Suction Only.* 4.1. *Maximum Mach Number Attainable.* As already explained, some diffuser suction can be obtained by rotating the 'bent' walls outwards about their rear end, thereby producing a gap between the trailing edge of the side perforated walls and the leading edge of the 'bent' walls. The maximum Mach number attainable in this way is usually limited by choking in the 'bent' wall section opposite the model support strut, or by having reached the maximum fan pressure ratio. Three geometric variables, therefore, have significant effect: the

size of the diffuser flap gap, the shape of the 'bent' walls and the angle of convergence of the side perforated walls. The effects of these variables are illustrated in Fig. 4.

Opening the diffuser-flap gap increases the maximum Mach number attainable. This would be expected since opening the gap increases the amount of diffuser suction and also, with the other variables constant, relieves the choking opposite the model support strut.

Only two alternative shapes of the 'bent' wall were investigated. In positions (1) and (2), the angle between the upstream and downstream halves of the 'bent' wall was 173½ deg and 176½ deg respectively. Position (1) gave the maximum attainable second throat area opposite the support strut. Position (2) gave rather less but was thought to be nearer the optimum setting for the higher supersonic speeds obtained with auxiliary suction. As expected, 'bent' wall position (1) delayed choking to higher Mach numbers than position (2). This can be seen from Fig. 4 and also from the following comparative values:

Values for M_{max}; walls parallel

Gap Size (in.) . . .	0	1·25	2·5
Bent wall position (1) .	0·91	0·99	1·05
Bent wall position (2) . .	0·88	0·95	1·00

Fig. 4 also shows that the maximum Mach numbers attainable can be improved by diverging the side porous walls, *e.g.*, an increase of about 0·05 for 24 to 36 minutes divergence. This is partly because with a given diffuser-flap gap size, diverging the porous walls means that the bent walls are further away from the support strut. Also, diverging the walls should reduce the amount of diffuser suction needed to achieve a given Mach number. These two reasons are not, however, the complete explanation. The centre-line Mach-number distributions in Fig. 8 show that with the walls diverged, a throat is formed just upstream of the working-section and the Mach numbers increase to a value near $M = 1 \cdot 1$, downstream of this throat. This supersonic expansion is, however, reflected at least twice further down the working-section, so the fact that higher Mach numbers can be achieved by diverging the walls is only of academic interest.

Converging the side porous walls causes choking at the downstream end of the working-section and because of this, irrespective of the gap size, Mach numbers greater than 0·9 cannot be reached.

With the porous walls parallel or diverged, the maximum Mach numbers attained with diffuser suction correspond to when choking occurs in the 'bent' wall section opposite the model support strut. This is illustrated in Fig. 5, which gives some typical Mach-number distributions* along the tunnel wall opposite the support strut for a set of conditions all corresponding roughly to when the maximum Mach number has been reached with the given wall geometry. The common feature between all these distributions is that a Mach number of between 1·05 and 1·10 has been reached at a point on the wall somewhere between the planes of the leading edge and the front shoulder of the strut. This is the section at which choking occurs.

---

* These Mach numbers are computed from the local static and working-section stagnation pressures, assuming isentropic flow. Strictly speaking, the Mach numbers quoted are incorrect owing to the total-head loss through the shock waves present in the 'bent' wall section. However, it is estimated that the resulting errors in Mach number should not be greater than 0·008, and consequently these errors do not affect the general argument.

Fig. 5 also shows that relatively high peak Mach numbers at the wall are attained just downstream of the trailing edge of the perforated plate for conditions when the diffuser suction flap is closed and the working-section Mach number is still subsonic. No corresponding peaks were observed in the centre-line distributions and it seems, therefore, that this local supersonic region cannot extend far out from the walls. It is presumably just a supersonic expansion around the corner which is produced by the different slope on the perforated and 'bent' walls. It was observed that this local supersonic region was formed before choking occurred, so it may be concluded that in general it is the section opposite the model support strut which produces choking rather than the section near the end of the perforated wall. The local supersonic expansion and subsequent compression is likely, however, to increase the boundary-layer thickness on the 'bent' walls, so it may have an indirect effect in producing choking opposite the support strut at a slightly lower Mach number.

4.2. *Centre-Line Mach-Number Distributions.* The centre-line Mach-number distributions with the perforated walls parallel and with the recommended flap gap sizes (*see* Section 4.3) are given in Fig. 6. It can be seen that up to $M = 1 \cdot 00$, the standard of uniformity over the test region, *i.e.*, the working-section length that would be occupied by a typical model, is extremely good. The variations in Mach number are within $\pm\ 0 \cdot 002$ and are almost within experimental error. They, therefore, satisfy the criterion that has sometimes been suggested for research tunnels. Also, no significant Mach-number gradients are present for Mach numbers up to $M = 1 \cdot 00$.

Above $M = 1 \cdot 00$, however, the standard of uniformity is not so good although, even for $M = 1 \cdot 05$, $\Delta M = \pm\ 0 \cdot 005$. This deterioration is, however, of only academic interest because tunnel operation with a model present in the working-section would not normally be possible at Mach numbers greater than $1 \cdot 00$ without the use of auxiliary suction.

It should be mentioned that the distributions plotted in Fig. 6 were obtained after some of the porosity modifications described in subsequent sections had been made. Referring to Fig. 3b, increase A and decrease A had already been incorporated. It is thought that the subsequent relatively minor increases B and C would have little effect on the Mach-number distributions for speeds up to $M = 1 \cdot 0$ and so the distributions in Fig. 6 can be taken as applying to the tunnel in its present state. Fig. 7 shows how the distributions for $M = 0 \cdot 95$ and $1 \cdot 0$ were affected by the porosity changes described as increase A and decrease A. It can be seen that these changes have had a beneficial effect in that the length over which the Mach number is closely uniform now extends far upstream of the model and into the flexible-nozzle section. Previously, with the original porosity distribution (Fig. 3a), the Mach-number distribution for $M = 1 \cdot 0$ only became level near where the nose of a typical model would be situated.

The centre-line Mach-number distributions with the walls diverged 24 minutes are given in Fig. 8. At subsonic speeds, there is now a positive static-pressure gradient through the level of the working-section which amounts to about $0 \cdot 01$ in Mach number over the length of a typical model; this is as would be expected from geometrical considerations. A deterioration occurs at supersonic Mach numbers because of the formation of a sonic throat ahead of the working-section followed by a supersonic expansion which is subsequently reflected down the working-section as already mentioned. The consequent variations in Mach number along the length of the working-section for $M = 1 \cdot 05$ are of the order of $\pm\ 0 \cdot 05$ and are therefore quite unacceptable.

4.3. *Fall-Off in Mach Number at the Rear of the Working-Section.* The most important feature needing careful attention at subsonic speeds is the position beyond which the Mach number falls off at the downstream end of the working-section. This is illustrated more clearly in Fig. 9 which shows that particularly for Mach numbers such as $0 \cdot 8$, this fall-off may start close to the tail of a model mounted in a typical position. This can be avoided by keeping the diffuser-flap gap closed but as already seen, it is necessary to open this gap to achieve Mach numbers greater than about $0 \cdot 9$ (or greater than about $0 \cdot 85$ with a model present in the working-section). Fortunately, as shown in Fig. 9, for a given gap size such as $2\frac{1}{2}$ in., increasing the Mach number from $0 \cdot 8$ to $1 \cdot 0$ has a decidedly favourable effect on the position of the start of the fall-off in Mach number: it is moved downstream by about 10 in. Once the gap is opened, further increase in the gap size does not cause any further appreciable upstream movement of the fall-off.

The precise form of the centre-line Mach-number distribution at the rear of the working-section at subsonic speeds is largely determined by two factors. First, there is the upstream influence of the flow field around the model support strut. This, at subsonic speeds, will result in a decrease in Mach number at the rear of the working-section. The second factor is the relative amounts of main-fan pressure ratio and of diffuser-suction mass flow that are being used to achieve a given Mach number. There is an optimum combination of these values which in the absence of the effect of the support strut, should give constant Mach number throughout the length of the working-section. This optimum combination will, of course, vary with test-section Mach number. If any given Mach number is achieved by using more suction and less fan pressure ratio than the optimum values, a fall-off in Mach number at the rear of the working-section would be expected and *vice versa*. These conclusions have been predicted theoretically and confirmed experimentally elsewhere. It is possible to interpret the present results on the basis of these effects. For example, with the gap closed and no auxiliary suction, it is likely that particularly for the higher subsonic Mach numbers, the pressure ratio across the fan is higher than the optimum referred to above. As the Mach number is increased, therefore, the tendency would be for the local Mach number to rise towards the rear of the working-section. This could explain the Mach-number distribution obtained for $M = 0 \cdot 9$, zero gap: the expansion that can be seen in this distribution is, therefore, due to an excess of fan pressure ratio and a deficit of suction while ultimately at the extreme rear of the working-section, the increase is replaced by a decrease because the influence of the support-strut flow field is then becoming predominant. Also, opening the diffuser-flap gap has the effect of increasing the suction and reducing the fan pressure ratio required to achieve a given Mach number, so the tendency will be for these values to lie on the other side of the optimum, particularly at the lower subsonic Mach numbers such as $M = 0 \cdot 8$. Hence, this factor, as well as the support-strut flow field, will both contribute to a reduction in Mach number at the rear of the working-section and this is in fact what is observed for $M = 0 \cdot 8$ and diffuser-flap gap opened. The arguments used above also explain why, for $M = 1 \cdot 0$, the fall-off in Mach number occurs at about the same position irrespective of whether the Mach number is achieved by diffuser suction, gap open, or auxiliary suction, gap closed.

This question of the fall-off in Mach number at the rear of the working-section should be carefully borne in mind when designing a new model and its supporting sting. It is best to be conservative in one's approach because tests elsewhere have shown that the presence of a model and its wake can move the start of the fall-off in Mach number quite appreciably upstream. Looking at Fig. 9, it may be tempting at first sight to say that no serious harm should result from having the tail of a model as far back as station 120 in. or possibly even further but such a conclusion would probably be unwise. It is not possible to make absolutely categoric recommendations because it depends on what is wanted from any particular model test. For the present, it seems fair to say that the rear of a model should not be behind station 115 in. and if possible, should be near or ahead of station 108 in. (*Note:* the end of the perforated plate is at station 146 in., *i.e.*, about, $0 \cdot 35h$ to $0 \cdot 4h$ downstream of the recommended model tail position.) It is worth recalling at this point that all the distributions presented here have been obtained with the model support strut in its central position (*i.e.*, strut leading edge at station 172·5 in.). Since the time of the calibration, the supporting strut has been moved 8 in. further back and as a result, it is probable that the fall-off in Mach number is also now occurring a little further downstream.

The general conclusion to be drawn from Fig. 9 is that with the tail of a model in a typical position such as station 108 in., the diffuser-flap gap should not be opened until this becomes necessary when a choked condition is reached. Even then, the aim should be to run with the minimum possible opening*.

Tests have shown that the gap opening required with a model present in the tunnel is, as would be expected, somewhat larger than that required in the tunnel, empty condition. As regards the maximum Mach number possible with a model present it has been found that this varies from about $M = 0 \cdot 94$ for a model having a blockage ratio of 0·5 per cent and set at an incidence giving a lift coefficient of about 0·8, to about $M = 1 \cdot 00$ for relatively small models.

4.4. *Summary of Results with Diffuser Suction only.* The results discussed above show that with the use of diffuser suction only, Mach numbers up to fairly near $M = 1 \cdot 00$ should be possible even when a model is present. The perforated walls should be set parallel and the diffuser-flap gap should be either closed or opened just enough to achieve the desired Mach number. Under these conditions, the centre-line Mach-number distributions in the empty tunnel should satisfy $\Delta M < \pm 0 \cdot 002$ and the fall-off in Mach number at the rear of the working-section should not start until downstream of about station 115 in.

5. *Results with Auxiliary Suction and With $M = 1 \cdot 0$ Nozzle.* As already noted, the Mach-number range in which supersonic flow is generated merely by auxiliary suction through the perforated wall, rather than by changes in the shape of the flexible nozzle, is from $M = 1 \cdot 00$ to about $M = 1 \cdot 12$.

5.1. *Centre-Line Mach-Number Distributions with Original Longitudinal Porosity Distribution.* The centre-line Mach-number distributions obtained with the perforated walls parallel and the original distribution of porosity (Fig. 3a) are given in Fig. 10. These were considered to be unsatisfactory because an appreciable over-expansion is evident at the upstream end of the working-section and also because the forward part of a model occupying a typical position in the tunnel would be in a region of accelerating flow for all Mach numbers greater than about 1·07. This is possibly not surprising since the nose of the model is assumed to be at only $0 \cdot 4 \times$ tunnel height downstream of the start of the perforated section.

Fig. 11 shows that altering the convergence angle of the side perforated walls does not provide a complete solution to these difficulties. A small amount of convergence reduces the over-expansion but on the other hand it makes the other difficulty worse, in that the final level Mach number is not attained until even further downstream. Quantitatively, it is found that converging the side

* This conclusion may not strictly apply for half-model testing when the support strut is no longer present. It may be necessary then to alter conditions so as to deliberately choke the tunnel at the rear of the working-section for the sake of maintaining reasonable stable flow conditions.

walls by 12 minutes, for example, reduces the amplitude of the over-expansion at $M = 1 \cdot 10$ from about $0 \cdot 03$ in Mach number to about $0 \cdot 02$ and further convergence to a total of 20 minutes reduces the amplitude to $0 \cdot 015$. However, for the same Mach number ($1 \cdot 10$), 24 minutes' convergence moves the start of the level part of the Mach-number distribution downstream by 10 in. from station 44 in. to station 54 in. This is quite unacceptable since the nose of some models may have to be as far forward as 37 in.

These results with the original porosity distribution showed, therefore, that changes would have to be made to the porosity distribution. Two types of change appeared necessary:

(1) In order to start the supersonic expansion from a point further upstream, an increase in porosity appeared desirable at the extreme forward end of the working-section.

(2) Changes to the subsequent porosity grading were required to control the rate of this supersonic expansion and thus if possible avoid the over-expansion.

These two problems are in fact just the same as those encountered when designing the initial slot shape for a slotted transonic working-section. In both cases, the problem is to generate the expansion to the desired supersonic speed as quickly as possible and yet to avoid any over-expansion which, if it occurs, will tend to reflect from the working-section walls further downstream and lead to a very poor standard of flow uniformity throughout the length of the working-section. With a slotted wall, this problem has been met by devising a slot shape having a fairly rapid rate of opening at this extreme upstream end, followed by a length in which its rate of opening is relatively slow; this in turn is succeeded by a length in which the slot width is increased fairly rapidly to its final value which is then left unchanged through the rest of the working-section. The middle transitional region in which the rate of opening is slow stabilizes the expansion and enables a higher rate of opening to be used further downstream.

It is perhaps not surprising that the modifications which were found to be necessary to the porosity distribution of the perforated walls of the A.R.A. tunnel have resulted in an open-area distribution which is quite closely similar to what other workers have found to be necessary for slots. The modifications introduced are shown in Fig. 3b. They were introduced in three stages and the effect of these stages will be considered separately. For the sake of convenience, all modifications were introduced on the side perforated walls, leaving the top and bottom walls unchanged. As will be realised from the detailed discussion later, it might have been better to make some modifications to the top and bottom walls.

5.2. *Effect of First-Stage Porosity Modifications.* The first stage of porosity modifications (Fig. 3b) consisted of:

(*a*) The increase A, which is an increase in the open-area ratio at the extreme upstream end of the perforated plate to a value of $7 \cdot 5$ per cent with this value being maintained over a distance of about 16 in. (Fig. 3b.)

(*b*) An upstream extension of the porosity forward on to the solid side walls by drilling some additional holes over a distance of about $19 \cdot 5$ in. ahead of the 0 in. datum. These extra holes were inclined at 60 deg to the normal; by this means, it is possible to reduce the number of holes required to achieve a given outflow to between $0 \cdot 25$ and $0 \cdot 35$ of the number that would be needed if the holes were drilled normal to the wall. The nominal open-area ratio of the inclined holes drilled in this region is about 2·6 per cent, so in terms of outflow, this should be equivalent to an open-area ratio of between 7·5 per cent and 10 per cent with normal holes.

The purpose of these two changes was to start the expansion to supersonic speeds from a point further upstream in the hope that thereby the Mach number would reach its final level value at a point in the working-section further forward than before. The Mach-number distributions obtained before and after these changes in porosity are compared in Fig. 12 for Mach number of 1·04, 1·08 and 1·10. It can be seen that the objectives have only been partly fulfilled. At $M = 1 \cdot 04$, the point beyond which the flow is reasonably uniform has been moved upstream from station 24 in. to station 4 in. but little improvement in this respect has been achieved at the higher Mach numbers. On the other hand, the magnitude of the over-expansion has been reduced from 0·01 to zero at $M = 1 \cdot 04$, from 0·02 to 0·015 at $M = 1 \cdot 08$ and from 0·03 to 0·022 at $M = 1 \cdot 10$.

The main interest here is in why the desired results have not been fully achieved at $M = 1 \cdot 08$ and 1·10, for example. It can be seen that at both these Mach numbers, the changes in porosity have, as expected, resulted in the flow expansion starting from a point further upstream, but the effect of this is practically eliminated by two subsequent compressions occurring at 14 in. and 30 in. at $M = 1 \cdot 08$ and at 15 in. and 35 in. at $M = 1 \cdot 10$ (Fig. 12). These compressions were not present in the original distributions and hence it is fair to assume that they are related to some feature on the modified side walls. By tracing back from the centre-line to the walls approximately along Mach lines, it was found that the first compression evidently originated from near the leading edge of the side perforated wall while the second compression originated from a point about 15 in. downstream of this. It appears likely, therefore, that the first compression is due to the effective discontinuity in the porosity distributions in between the inclined holes as drilled in the solid wall (where the effective open area ratio is about 7·5 per cent), and the station 6 in. downstream of datum where the open-area ratio of the perforated plate reaches 7·5 per cent: in between these two stations, the effective porosity is nearer zero than 7·5 per cent. Similarly, the second compression can possibly be attributed to insufficient open-area ratio in a limited region between about station 15 in. and station 20 in., *i.e.*, just ahead of where the perforations on the horizontal walls start. Alternatively, the second compression may be related to errors in slope or slight mismatching of the solid and perforated floors, both in the vicinity of the saw-teeth junction (this is known to be troublesome at higher Mach numbers).

It thus appears that there is a strong correspondence between the centre-line Mach-number distributions and the local wall-porosity distributions, this correspondence being effected along lines at approximately the Mach angle. Strictly, it is probable (and detailed evidence in support of this was found during the tests), that compressive disturbances are propagated at more than the Mach angle and expansive disturbances at rather less than the Mach angle, corresponding to the mean Mach number of the stream. As seen above, both what has been achieved with the stage 1 porosity modifications and also what is still wrong with the distributions can be explained on the basis of this local correspondence. In other words, changing the open area at an arbitrary station X results in a change in the Mach number on the centre-line at the station where the Mach line from X crosses it but not at stations downstream of this. This may appear to be a simple and possibly self-evident result but nevertheless, it was not appreciated prior to making these stage 1 porosity modifications.

Even although these stage 1 changes did not fully achieve the desired results, the general conclusion is that they were nevertheless worth while. It is probable that the changes described later would not otherwise have been so effective and quite apart from the Mach-number range at present being discussed, the stage 1 changes helped at subsonic speeds (*see* Section 4.2) and at off-design Mach numbers at the higher supersonic speeds (*see* Section 6.2).

One minor point shown in Fig. 12 is also worth mentioning. The distribution for $M = 1 \cdot 04$ shows that a compression wave is being reflected at intervals of about 20 in. along the working-section. This interval corresponds to a reflection from the horizontal walls and it seems that the origin of the disturbance is near station 23 in. The origin is, therefore, possibly once again near the saw-teeth junction on the floor (or roof). All trace of this disturbance is lost at the higher Mach numbers: this is possibly because it is masked by the other compressions and expansions then present. Another possible explanation is that the effectiveness of the perforated wall in eliminating reflections of incident disturbances, particularly compressions, steadily improves as the Mach number is increased beyond $M = 1 \cdot 0$ and hence for this reason, the recurrent perturbation might be less evident at, say, $M = 1 \cdot 08$ than at $M = 1 \cdot 04$.

5.3. *Effect of Second and Third-Stage Porosity Modifications.* The results obtained from the stage 1 modifications and the analysis of them, leading to the correspondence principle discussed above show that to reduce the over-expansion still further and also to ensure that the Mach number near the nose of a typical model is already up to near the value applying through the rest of the working-section, it is necessary to reduce the open-area ratio between about station 20 in. and station 50 in. The decrease A shown in Fig. 3b was, therefore, tried. Together with this decrease, the open-area ratio was increased locally between station 13 in. and station 18 in. (increase B) in an attempt to eliminate the second compression referred to above. These two modifications are called the stage 2 modifications. As will be seen from Fig. 3b, combining the new open-area ratio distribution on the side walls with the one already existing on the top and bottom walls now gives an average open-area distribution of the form suggested earlier, *i.e.*, an initial relatively rapid increase followed by a long fairly flat portion, followed in turn by the relatively rapid rise to the final basic value of $22 \cdot 5$ per cent.

Fig. 13 compares the centre-line Mach-number distributions obtained before and after the stage 2 modifications. The over-expansion amplitudes were reduced from $0 \cdot 013$ in Mach number to zero at $M = 1 \cdot 07$, from $0 \cdot 018$ to $0 \cdot 012$ at $M = 1 \cdot 08$ and from $0 \cdot 022$ to $0 \cdot 012$ at $M = 1 \cdot 10$. The absolute values of the amplitudes after the modifications should perhaps be treated with caution because they are now of the order of the scatter due to a combination of centre-line static-tube errors and of other disturbances in the flow. The second compression referred to above was also appreciably alleviated at $M = 1 \cdot 10$ but this effect could still be seen at the lower Mach numbers.

It can be concluded therefore that the drastic modification in porosity labelled decrease A has had the desired effect in materially reducing the over-expansion to tolerable values for Mach numbers up to $1 \cdot 10$. On the other hand, some change is still desirable in order to increase the Mach number obtained near the nose of a typical model to a value nearer that achieved over the rest of the test section. This latter difficulty is at least partly due to the fact that the second compression has not been completely eliminated by the increase B, so a further increase (increase C, Fig. 3b) was tried in this region. The combination of increase B and increase C means that the local increase in porosity in this region now extends from station 13 in. to station 20 in. on the side wall (*N.B.* the perforated plate on the top and bottom walls starts at station 20 in.). At the same time, to eliminate any possible adverse downstream effects of the first compression, an additional vertical row of inclined holes was drilled in the saw teeth of the side walls in order to smooth out the discontinuity in the porosity distribution. These further two changes, *i.e.*, increase C and the extra inclined holes, are referred to as the stage 3 modifications and the centre-line Mach-number distributions obtained before and after these changes are compared in Fig. 14.

The comparison shown in Fig. 14 is complicated by the fact that it is not possible to compare curves at precisely the same M_{plenum}. For example, comparison is made between the results for $M = 1 \cdot 112$ before the stage 3 modifications and for $M = 1 \cdot 119$, after modification. These differences in Mach number may appear small but it should be noted that in this Mach-number range between $1 \cdot 08$ and $0 \cdot 12$, very significant changes in the uniformity of the centre-line distributions over the test section occur as the Mach number is increased. Strictly, for purposes of comparison, the general levels of Mach number on any curves being compared should not differ by more than about $0 \cdot 003$. However, Fig. 14 shows that, presumably because of increase C, the magnitude of the first compression has been reduced and also, the Mach-number distributions appear to be somewhat smoother near station 60 in. This may be because a reflection of either the first or second compression has been alleviated. It seems that the combined increase B and increase C has been at least partly effective in that the Mach number near the nose of a typical model is now near the value obtained further downstream.

Even after the stage 3 modifications, Fig. 14 shows that some over-expansion is still tending to occur at the higher Mach numbers between stations 60 in. and 75 in. An attempt was made to reduce this further by blocking up some of the holes in the side wall between stations 38 in. and 48 in., *i.e.*, decrease B in Fig. 3b. This produced little improvement, however, and merely shifted the over-expansion somewhat further downstream without reducing its amplitude.

Another small disturbance in the distributions is a compression which appears to cross the centre-line near station 86 in. at $M = 1 \cdot 081$ and station 94 in. at $M = 1 \cdot 096$. A possible explanation for this disturbance is that it originates from station 68 in. on the side wall where, as can be seen from Fig. 3b, the approximately linear grading in porosity up to the value of $22 \cdot 5$ per cent ends quite abruptly.

From these last comments, it would seem some further minor refinements in the open-area distribution could lead to improvements in the flow uniformity for Mach numbers between $M = 1 \cdot 09$ and $M = 1 \cdot 12$. If, for convenience, these were again incorporated on the side walls, a possible change would be to include decrease B but then to increase the open-area ratio from 5 per cent to $22 \cdot 5$ per cent somewhat more gradually, taking care to fair off this part of the curve both where it fairs into decrease B and where it fairs into the final value of $22 \cdot 5$ per cent. This suggestion is shown in Fig. 3b as the possible change D. This would mean that the final value of the open-area ratio was not achieved until some point downstream of station 68 in. More logically, what is probably required is that the open-area distribution on the top and bottom walls should be modified to a shape more similar to what has been incorporated on the side walls. The faults originating from stations between about 40 in. and 68 in. are probably due to the rapid, nearly linear increase in open-area ratio on the top and bottom walls (Fig. 3a). Better distributions would probably have resulted if there had been a flat stabilizing region similar to that introduced on the side walls.

Up till the present in this Section, all the discussion has been concerned with the distributions obtained with the side perforated walls parallel. As will be shown below, converging these walls has quite a significant effect on the flow development and hence it was felt that before any final minor refinements were made to the porosity distributions, it was best to wait until analysis of model tests had shown whether converging the side walls helps materially to improve the reflection-wave attenuating properties of the perforated wall. Accordingly, even although, as just described, ways are known for possibly improving still further the Mach-number distributions, walls parallel, no further steps in this direction have yet been taken.

5.4. *Effect of Wall Convergence with the Final Open-Area Distributions.* In general, the effect of converging the side walls with the final open-area distribution was found to be similar to that already shown for the original porosity distribution. Converging the walls tended to decrease any over-expansion at the expense of moving downstream the point beyond which the uniform Mach number became established.

The Mach-number distributions obtained with different amounts of convergence are shown in Fig. 15a for $M = 1 \cdot 04$ and $M = 1 \cdot 06$, in Fig. 15b for $M = 1 \cdot 08$ and in Fig. 15c for $M = 1 \cdot 10$.

At $M = 1 \cdot 04$ and $1 \cdot 06$, converging up to 12 minutes does not cause any serious deterioration but at the higher Mach numbers or with larger amounts of convergence, the Mach-number distributions were not as good as with walls parallel, largely because the nose of a typical model would be in the region where the Mach number is still increasing up to its uniform value.

For $M = 1 \cdot 10$, comparative values are given below:

Wall configuration	$M_{\text{model nose}}$	$M_{\max}$	$M_{\min}$	$M_{\text{model tail}}$	ΔM
Parallel . . .	1·090	1·103	1·085	1·105	±0·009
Converged 6 minutes.	1·085	1·103	1·090	1·102	±0·009
Converged 12 minutes	1·072	1·105	1·072	1·100	±0·012

The above values show that with the final open-area distributions, convergence by more than 6 minutes is not possible for Mach numbers such as 1·10 unless a relatively short model placed well back in the working-section is being tested. Detailed analysis of the results suggests that the second compression referred to earlier as originating from near station 20 in. is still quite a contributory factor to the poor distributions obtained with walls converged. It is difficult, however, to see how the open-area ratio could safely be increased on the side walls in this region beyond what has already been done in increase B and C so, if it is later found to be important to try and obtain better distributions with walls converged, some alteration to the porosity distribution on the top and bottom walls may have to be included, *i.e.*, a change on these walls comparable with increase A on the side walls.

Any divergence of the side perforated walls merely aggravates the tendency for an over-expansion to occur and for this over-expansion to be reflected from the working-section walls, thus giving a very poor standard of flow uniformity throughout the length of the working-section. Also, it was found that the airflow was distinctly less steady with the walls diverged, presumably because of the thicker boundary layer on the walls. No Mach-number distributions have therefore been presented to show the effects of diverging the walls.

5.5. *Concluding Remarks on Final Distributions.* For ease of reference and detailed analysis, the Mach-number distributions obtained in the region of the model with walls parallel are reproduced to a larger scale in Figs. 16a, 16b and 16c. These are results from measurements on the alcohol manometers. Some slight differences may be noted between these distributions and those plotted in the earlier Figures. This is because the values given in Fig. 16 were obtained from the lower rather than the upper tappings on the centre-line static tube. The change has been made because these lower tappings were connected to the alcohol manometers, thus giving a greater accuracy. Some of the scatter shown in the distributions of Fig. 16 can possibly be attributed to static-tube errors as discussed earlier. The change in scale between Fig. 16 and earlier Figures should also be noted: in Fig. 16, one large division represents $0 \cdot 05$ in Mach number.

The general conclusions to be drawn from these final distributions are:

(*a*) Apart from a few isolated points, the distributions with walls parallel can be counted as quite satisfactory for Mach numbers up to and including $1 \cdot 08$. In this Mach-number range, ΔM is less than $\pm 0 \cdot 005$.

(*b*) With further increase in Mach number beyond $M = 1 \cdot 08$, the two original faults of some over-expansion and the final uniform Mach number being reached rather too far downstream still apply but to a much smaller extent than with the original distributions. The maximum irregularities over the length of a typical model increase to about $\pm 0 \cdot 006$ at $M = 1 \cdot 093$, $\pm 0 \cdot 009$ at $M = 1 \cdot 112$ and $\pm 0 \cdot 011$ at $M = 1 \cdot 119$. Aft of station 50 in., the corresponding values are only $\pm 0 \cdot 004$ at $M = 1 \cdot 093$ or $\pm 0 \cdot 007$ at $M = 1 \cdot 119$. These values are considerably better than with the original open-area distribution for which, for example, the irregularities amounted to $\pm 0 \cdot 015$ at $M = 1 \cdot 106$.

(*c*) With a full-length model having its nose somewhere near station 40 in., it seems quite fair to accept test results up to $M = 1 \cdot 095$. With shorter models, results at even $M = 1 \cdot 12$ should be all right. Tests on actual models suggest that these statements are probably conservative. Another way of expressing this conclusion is that for $M = 1 \cdot 095$, only about $0 \cdot 4 \times$ tunnel heights downstream of the flexible plate (*i.e.*, start of the perforated plate), is required to establish the flow. This compares very favourably with experience elsewhere.

(*d*) As already suggested, still further improvements in the Mach-number distributions should be possible if these are thought to be necessary. With walls parallel, the most useful change would probably be that suggested in Section 5.3, *e.g.*, change D on Fig. 3b.

(*e*) To obtain better distributions with walls converged, it will undoubtedly be necessary to make some changes near station 20 in. in order to ensure that the Mach number near the model nose is nearer to the value applying over the rest of the model.

(*e*) Since the calibration described here has been completed, the model support strut has been moved 8 in. further rearward so that the 'nose and tail of typical models' will also be 8 in. further back, as compared with the positions marked on most of the distributions (*see* Fig. 16). The chief object of this move was to help to ensure that for Mach numbers such as $1 \cdot 10$, $1 \cdot 12$, the stream Mach number near the model nose was not significantly less than for the rest of the model. The figures for flow uniformity are therefore now slightly better than those quoted above.

6. *Results with Auxiliary Suction in Combination with the Supersonic Nozzles.* As explained earlier, it is possible to set the flexible nozzles on the top and bottom walls to give shapes nominally corresponding to working-section Mach numbers of 1·15, 1·20, 1·25, etc. For Mach numbers of 1·15 and above, therefore, the supersonic flow is basically generated by the flexible nozzle and the auxiliary suction is used to pull the terminal shock wave back to near the end of the perforated plate, to produce a reasonably uniform Mach-number distribution through the working-section, to reduce the thickness of the boundary layer on the walls and to provide some measure of cancellation of reflected waves. To some extent, the auxiliary suction can be considered as increasing the effective pressure ratio across the working-section; some exchange between this pressure ratio and that provided by the main fan is possible without altering the centre-line Mach-number distribution. However, there is still a certain main-fan pressure ratio below which supersonic flow at a given Mach number cannot be maintained, whatever the auxiliary-suction mass flow. If the fan pressure ratio is reduced below this critical value, the flow breaks down as it would in a conventional convergent-divergent nozzle. With the pressure-ratio available in the A.R.A. tunnel, it has been found possible to operate the tunnel with the $M = 1 \cdot 4$ nozzle shape and by using an appropriate amount of auxiliary suction to achieve a maximum Mach number, tunnel empty, of $M = 1 \cdot 43$. Operation with the next flexible nozzle setting corresponding to $M = 1 \cdot 5$ has not been tried but is not likely to be possible owing to insufficient fan pressure ratio.

The general procedure adopted when running the tunnel at these supersonic Mach numbers is to select a fan pressure ratio just greater than the critical value, and then to carry out the final adjustment of Mach number by regulating the auxiliary suction. With an appropriate amount of suction, it is possible to have the mean Mach number through the working-section approximately equal to the Mach number at the downstream end of the nozzle. When the suction and the nozzle setting are matched in this way, it is said that the tunnel is operating at one of its design Mach numbers and the centre-line Mach-number distributions should then be the best possible. If larger suction quantities are used, it is of course possible to achieve Mach numbers in the working-section higher than that at the end of the flexible nozzle but at the expense, as will be seen later, of somewhat poorer Mach-number distributions. If the suction quantity is reduced significantly below that needed for the design case, the flow through the working-section breaks down and the terminal shock moves forward to the end of the flexible nozzle. This process happens quite suddenly, particularly when no model is present in the working-section but the wall pressures usually give some warning that it is about to happen. Under the design conditions, except possibly at $M = 1 \cdot 4$, the terminal shock intersects the wall near the end of the perforated plate; if the suction quantity is then reduced, the terminal shock moves slowly forward by about 6 in. before it suddenly flicks forward to the end of the nozzle. This, in fact, illustrates the reason for the instability of the phenomena: when the shock is lying ahead of the end of the perforated plate, there will be some outflow through the wall at the rear of the working-section behind the shock. This would ultimately imply an inflow into the working-section ahead of the shock but this is impossible if the Mach number is to be maintained, so the only physical solution is for the shock wave to jump to the forward end of the perforated plate.

In the following discussion, consideration is given first to the centre-line Mach-number distributions obtained, perforated walls parallel at the Mach numbers corresponding approximately to the nozzle-design Mach numbers. These distributions are analysed to find the source of the disturbances present on the centre-line and it is shown how during the calibration they were improved by various realignments and adjustments to the walls. The 'off-design' Mach-number distributions are presented in Section 6.2 for the walls parallel case and then, in Section 6.3, the effects of converging or diverging the perforated walls, which provide another method for obtaining 'off-design' Mach numbers, are discussed briefly.

6.1. *Centre-Line Distributions at Nozzle-Design Mach Numbers, Perforated Walls Parallel.* The centre-line Mach-number distributions obtained at a relatively early stage in the calibration are shown in Fig. 17 for Mach numbers of $1 \cdot 20$, $1 \cdot 30$ and $1 \cdot 40$. These original distributions do not satisfy the desired standards of flow uniformity, this being particularly true at the higher Mach numbers. Analysis of the disturbances present in the distributions for the higher Mach numbers showed that if these were traced back to the walls along the Mach lines, the apparent origins of the disturbances were at roughly the same positions, irrespective of Mach number. For example, the compression labelled A appeared to originate from near the last jacking station in the flexible nozzle, the disturbances B from near the saw-teeth joints on the side walls and the disturbances C from near the saw-teeth joints on the top and bottom walls. Detailed investigations of the geometry of the wall and of the joints between solid and perforated walls were made leading to various realignments and adjustments of the walls. Significant improvements in the centre-line distributions resulted as shown by the comparisons in Fig. 17. These realignments were made simultaneously with some of the changes in porosity distributions discussed in Section 5 but it was established that at the design supersonic Mach numbers, the changes in porosity distribution had very little effect on the centre-line Mach-number distributions.

To assist in the analysis of the disturbances, Fig. 18 has been produced to compare the centre-line distributions obtained with the tube in its normal position and with it rotated through 180 deg in order to obtain an indication of whether the disturbances originate from the side, upper and/or lower walls. Also shown are the loci of Mach lines from various selected points. These distributions were obtained at a fairly late stage in the calibration when most of the adjustments and realignments had been made.

Fig. 18 shows clearly that the predominating disturbances in the test region originate from near the saw-teeth junctions, particularly on the floor. Considering the distributions for $M = 1 \cdot 35$, for example, the disturbances between about stations 43 in. and 56 in. are probably related to the saw-teeth junction on the side walls and the more serious disturbances between stations 56 in. and about 73 in. are from the top and bottom walls. Results at $M = 1 \cdot 25$, $1 \cdot 30$ and $1 \cdot 40$ all suggest that the floor is more serious than the roof since the disturbances in the 'lower' position are stronger and displaced upstream relative to those in the 'upper' position, this displacement being a result of the finite thickness of the centre-line static tube. This latter conclusion is not surprising because the central part of the floor would be expected to be the more difficult to fit perfectly since it is removable to allow for installation of the solid floor which serves as a reflection plate for half models. This part of the floor was actually removed and replaced several times during the calibration and it was found that this could alter quite markedly the magnitude and precise form of the appropriate disturbances in the centre-line Mach-number distribution. Because the precise distributions were so sensitive to apparently minor changes, it is perhaps pointless to discuss them in detail but it seems that usually, the disturbance originating from the floor saw-teeth junction consists of an expansion followed by a compression and subsequent expansion; this is, for example, quite evident in the curves for $M = 1 \cdot 35$ in Fig. 18. It is worth adding that the trouble may not be merely related to bad fits near the apices of the saw teeth. It is believed that the actual slope of the floor over the length of the saw teeth is slightly different from the slope existing either ahead of or behind this region. This change of slope is such that there is usually a convex corner at the upstream end and a concave corner at the downstream end. Qualitatively, these changes are consistent with the effects in the observed centre-line distributions. Particularly in view of the need to remove part of the perforated floor every time a half model is being tested, it seems impracticable to expect that any great material improvement can be made in this region, so it would be difficult to obtain a better standard of flow uniformity in the region between stations 55 in. and 70 in. at Mach numbers of $M = 1 \cdot 30$ and above. It is noteworthy, however, that the disturbances from the saw-teeth junctions are relatively minor at Mach numbers below $1 \cdot 30$ and this would certainly not have been the case if there had been a straight junction, normal to the stream, between the flexible nozzle and the perforated plate: experience in other tunnels has shown that it is quite easy to get a perturbation of $0 \cdot 02$ in Mach number from a straight joint at $M = 1 \cdot 2$. Despite the irregularities at $M = 1 \cdot 3$ and above, therefore, it can certainly be said that the saw teeth have justified themselves.

Fig. 18 also shows the characteristics of the flow that can be related to the shape of the rear part of the flexible nozzle. It can be seen that there is no consistent evidence indicating any asymmetry in the nozzle shape, *i.e.*, unforeseen compressions and expansions seem to be produced equally from both walls rather than only from one. Certainly, considering the flow between the Mach lines from jacking stations 3 and 1, there is a change as the Mach number is increased from $M = 1 \cdot 20$ to $M = 1 \cdot 40$ from a regime in which the Mach-number gradient is positive to one in which the gradient is negative. The consistent smooth variation in trend as the Mach number is increased would suggest some consistent weakness in the assumptions or methods used in designing the nozzles rather than errors in the actual manufactured shapes and it has indeed been checked that manufacturing errors are relatively slight. It is difficult to know whether these actual changes in Mach number matter or not. Even at $M = 1 \cdot 40$, the flow is essentially free of gradients* downstream of the position corresponding to a typical model nose, so the only reason for concern is that these compressions or expansions must reflect to some extent from the walls and these lead to some of the irregularities in the rear part of the working-section.

The final centre-line Mach-number distributions obtained in the region of a typical model, perforated walls parallel, for the design Mach numbers are given in Fig. 19. These distributions are almost the same as those previously given in Fig. 18, except that small differences in the porosity distributions have been made. Both 'upper' and 'lower' distributions are given.

The Mach-number scatter bands† in the test region (assumed to be about 6-ft long) are given in the following Table:

Nozzle .	$1 \cdot 15$	$1 \cdot 20$	$1 \cdot 25$	$1 \cdot 30$	$1 \cdot 35$	$1 \cdot 40$
M_{design} .	$1 \cdot 140$	$1 \cdot 194$	$1 \cdot 246$	$1 \cdot 299$	$1 \cdot 350$	$1 \cdot 396$
$\pm \Delta \bar{M}$.	$0 \cdot 009$	$0 \cdot 0075$	$0 \cdot 010$	$0 \cdot 011$	$0 \cdot 012$	$0 \cdot 016$

* The apparent Mach-number gradients between stations 70 in. and 100 in. at some of the Mach numbers are due to the working-section Mach numbers being slightly higher than the Mach numbers at the end of the nozzles; these gradients can therefore be removed by slightly reducing the auxiliary-suction quantities.

† The values quoted may err on the conservative side because they include possible tube errors and other measuring errors.

These values were obtained by averaging the values for the upper and lower tappings. The trend, as one would expect, is for the scatter band width generally to increase with Mach number. The unexpectedly large scatter for the $M = 1 \cdot 15$ nozzle is almost entirely due to the positive Mach-number gradient existing towards the rear of the test region for this case. It will be shown later that this gradient can be reduced by converging the side walls very slightly: this is discussed in more detail in Section 6.3.

It may be felt that the values given in the Table above do not give quite the same impression as is obtained by looking at the distributions in Fig. 19. The plotted distributions suggest a more serious deterioration with increasing Mach number than implied in the figures in the Table or, more correctly, that the distributions for the lower Mach numbers such as $1 \cdot 20$ are rather better than the Table would suggest. This appears to be a fair comment because it is broadly true that the magnitude of the scatter bands for the lower Mach numbers are determined primarily by gradients through the test region whereas at the higher Mach numbers, they are determined by the magnitude of actual disturbances crossing the region. If the fault is due to a gradient, there is always hope that it can be removed by changing the wall angle or, alternatively, that corrections such as buoyancy corrections can be made to allow for some of the consequences. On the other hand, corrections obviously cannot be made to allow for the effect of isolated disturbances of the wall crossing a model in the test section.

As already explained, some of the trouble at the higher Mach numbers is due to the disturbances originating from near the saw-teeth junction in the floor. If the model being tested is relatively short, it can be placed in the rear part of the working-section so that its nose is behind these particular disturbances even at the highest Mach number. In such cases, the order of the flow uniformity would be significantly better as shown by the values in the following Table:

Nozzle .	$1 \cdot 15$	$1 \cdot 20$	$1 \cdot 25$	$1 \cdot 30$	$1 \cdot 35$	$1 \cdot 40$
$\pm \Delta \bar{M}$.	$0 \cdot 009$	$0 \cdot 005$	$0 \cdot 005$	$0 \cdot 007$	$0 \cdot 007$	$0 \cdot 007$

The best case of all would be an intake model where it is probably only necessary to achieve a uniform Mach-number distribution over a relatively short length of the working-section.

Despite the reservations made regarding the flow uniformity at the highest test Mach numbers, it is considered that the standards achieved are reasonably good. If occasion offers, however, an attempt will be made to improve the distributions for $M = 1 \cdot 3$ and above.

6.2. *Off-Design Centre-Line Mach-Number Distributions, Perforated Walls Parallel.* As mentioned earlier the working-section Mach number can be increased above the design value for any nozzle, by increasing the auxiliary-suction quantity. An obvious limitation to this approach is that the extra auxiliary suction will not affect the flow on the centre-line upstream of the Mach line from the leading edge of the start of the porosity and that the Mach number on the centre-line will then continue to increase slowly for some distance downstream of this. This implies that use of this method is not possible for Mach numbers greater than about $1 \cdot 20$ unless a very short model or particularly an intake type of model is being tested. The modifications made to the original porosity distributions have of course helped in this respect. This is particularly true of the increase A which included the drilling of some inclined holes in the solid side walls ahead of the perforated plate. This ensured that the increase in Mach number started from a point further upstream: a comparison of the distributions obtained for off-design Mach numbers using the $M = 1 \cdot 15$, $1 \cdot 20$ and $1 \cdot 25$ nozzles confirmed that these porosity changes had been beneficial.

Fig. 20 shows the effect on the centre-line Mach-number distributions of increasing auxiliary suction with the $M = 1 \cdot 15$, $1 \cdot 20$ and $1 \cdot 25$ nozzles. At $M = 1 \cdot 16$, the uniform Mach number applying through the rear part of the working-section has been reached ahead of the probable model position and the standard of uniformity downstream of this is virtually as good as for the design case at $M = 1 \cdot 14$. At the off-design conditions with the $M = 1 \cdot 2$ and $1 \cdot 25$ nozzles, the start of the flow acceleration occurs further downstream and the trend is for there to be a positive Mach-number gradient over the forward part of a typical model followed by a limited reduction in Mach number near the tail of the model. The main conclusion from Fig. 20 is that for Mach numbers above $M = 1 \cdot 16$, the uniformity of the centre-line Mach-number distributions is quite sensitive to departure from the design condition and it is, therefore, important to note what are the precise design Mach numbers, as distinct from their nominal values. The actual values appear to lie near $M = 1 \cdot 14$, $1 \cdot 19$, $1 \cdot 24_5$, $1 \cdot 30$, $1 \cdot 35$ and $1 \cdot 39$. These values would not necessarily apply precisely if there were a large model in the working-section.

It is also worth noting that the design conditions refer to when the working-section Mach number is about the same as the Mach number produced by the nozzle rather than some absolute value of Mach number. It has been found that if the air is not sufficiently dry, condensation shocks result in a lower Mach number being produced by the nozzle and in such circumstances, the auxiliary suction should strictly be adjusted to give a correspondingly lower Mach number in the working-section. If this is not done, a serious deterioration in flow uniformity would result. This is actually one of the more important reasons for imposing strict standards of dryness. In practice, it has been found necessary to keep the relative humidity below $0 \cdot 001$ lb water/lb air.

6.3. *Effect of Perforated-Wall Convergence on the Centre-Line Mach-Number Distributions.* If the perforated side walls are converged, there is a change in slope at some point on the solid side wall inside the flexible nozzle and a fan of compression waves originates from this region, thus reducing the Mach number below the value that would otherwise be produced by the flexible nozzle. One possible use, therefore, of wall convergence would be to obtain off-design Mach numbers, provided that the compressive disturbances were not reflected from the walls in the working-section, thus giving a poor Mach-number distribution. Also, if the walls are converged, the boundary-layer thickness on the walls is smaller for any given Mach number than if the walls were parallel and because of this, it is thought that converging the side walls may assist in the alleviation of shock-wave reflections. Another possible application of convergence, as already mentioned, is to try to eliminate the positive Mach-number gradients present in the region of the model at such Mach numbers as $1 \cdot 15$ with the walls parallel.

Some typical Mach-number distributions obtained with the side walls converged slightly are shown in Figs. 21, 22 and 23. It can be seen that the magnitude of the initial compression at the forward end of the working-section increases with increasing convergence. The apparent impression that there are two compressions in succession in some of the distributions is probably misleading: it is likely that two effects are being superimposed because it can be seen from the distribution for $M = 1 \cdot 14$, walls parallel, for example, that an expansion system is present in the same region on the centre-line and this probably persists whether the side walls are converged or not.

The first conclusion that can be drawn from these distributions is that using about six minutes' convergence with the $M = 1 \cdot 15$ nozzle gives a rather better standard of flow uniformity at or near the design Mach number, than was obtained with the walls parallel, *e.g.*, for $M = 1 \cdot 153$, six minutes' convergence, $\Delta M = \pm 0 \cdot 006$ as compared with $\Delta M = \pm 0 \cdot 009$ for $M = 1 \cdot 14$, walls parallel. This improvement is because this small amount of convergence has been effective in largely removing the positive Mach-number gradient that exists through the test region when the walls are parallel. With the $M = 1 \cdot 2$ nozzle, converging by six minutes also tends to remove a positive gradient but the scatter band is virtually the same as with the walls parallel, *i.e.*, $\Delta M = \pm 0 \cdot 0075$.

The second interesting conclusion is that although converging the side walls enables one to obtain Mach numbers below the design Mach number of the nozzle, this is done with a reduced standard of flow uniformity. For the walls parallel case, it was found that the best distributions were obtained when M_{plenum} was about the lowest possible for any given nozzle shape but it now appears that this conclusion no longer applies when the walls are converged. It is then better to operate at a Mach number somewhat higher (perhaps as much as $0 \cdot 02$ higher), than the minimum possible with that particular nozzle and amount of wall convergence. There are various examples of this general statement, *e.g.*,

(*a*) In Fig. 21, the distribution for $M = 1 \cdot 153$ with six minutes' convergence is rather more uniform than the distribution for $M = 1 \cdot 130$. This is because the additional auxiliary suction required to obtain $M = 1 \cdot 153$ is effective in raising the Mach numbers near station 40 in. and so in helping to eliminate the effects of the rear half of the fan of compression waves.

(*b*) The distribution for $M = 1 \cdot 133$, 12 minutes' convergence in Fig. 21 is better than that for $M = 1 \cdot 115$ in Fig. 22.

(*c*) The distribution for $M = 1 \cdot 124$, 24 minutes' convergence in Fig. 22 is better than that for $M = 1 \cdot 115$, 12 minutes' convergence: this is because it would be quite easy with 24 minutes' convergence to obtain a Mach number as low as $1 \cdot 10$, so the distribution for $M = 1 \cdot 124$ already includes the improvement that can be obtained by running at a Mach number rather higher than the minimum.

It follows therefore from this second conclusion that the use of convergence to obtain off-design Mach numbers is not as satisfactory as might at first have been expected. With a small amount of convergence such as six minutes, it is best to continue to run at the nozzle-design Mach number and if a larger amount of convergence such as 24 minutes is used, it is best to run at a Mach number, still only perhaps $0 \cdot 01$ to $0 \cdot 02$ below the value that would have been chosen with walls parallel.

The third conclusion from the distributions obtained with walls converged is that even if the optimum Mach number is carefully chosen for the particular amount of wall convergence, there is a significant deterioration in flow uniformity if the walls are converged by more than about 6 minutes. Expressed as a scatter band, with the $M = 1 \cdot 15$ nozzle, there is a deterioration from $\Delta M = \pm 0 \cdot 006$ at $M = 1 \cdot 153$, 6 minutes' convergence to $\Delta M = \pm 0 \cdot 012$ for $M = 1 \cdot 124$, 24 minutes' convergence. Similarly, with the $M = 1 \cdot 2$ nozzle, there is a deterioration from $\Delta M = \pm 0 \cdot 008$ for $M = 1 \cdot 188$, 6 minutes' convergence to $\pm 0 \cdot 012$ for $M = 1 \cdot 80$, 12 minutes' convergence*. It

* The distributions given in Fig. 23 for the $M = 1 \cdot 2$ nozzle are the best of those obtained with either 6 minutes' or 12 minutes' convergence.

would be wrong, however, to think of this deterioration as scatter: with the walls converged more than 6 minutes and the $M = 1 \cdot 15$ nozzle, there tends to be a positive Mach-number gradient over the forward half of the model (*i.e.*, back to about station 80 in.) followed by a negative gradient over the rear half. The positive gradient is presumably partly associated with the additional auxiliary suction being used to achieve the given Mach number. The negative gradient over the rear of the working-section may either be a reflection of the incident compression fan or alternatively it is merely a consequence of the auxiliary suction having produced an over-expansion near station 80 in. It is clear that the increase in Mach number from $1 \cdot 15$ to $1 \cdot 20$ makes it more difficult to obtain a satisfactory distribution with walls converged more than 6 minutes. This is largely because, as might be expected, the positive Mach-number gradient now extends to near station 100 in. rather than station 80 in. Consequently, more of the model would tend to be in the region of a positive Mach-number gradient and it is clear that if the walls were converged with the $M = 1 \cdot 25$ nozzle, the whole model would be in a region of positive gradient.

Summarising the possible usefulness of converging the side walls, it can be said that at Mach numbers greater than $1 \cdot 2$, no convergence is permissible; with the $M = 1 \cdot 2$ nozzle, it is undesirable to use more than 6 minutes' convergence; and with the $M = 1 \cdot 15$ nozzle, 5 minutes' convergence improves the standard of flow uniformity at the design Mach number and up to about 12 minutes' convergence or even possibly 24 minutes' convergence can be used to obtain Mach number in the range between $1 \cdot 10$ and $1 \cdot 15$. On this last point, it is interesting to note that the comparison in Fig. 22 shows that for $M = 1 \cdot 12$, it is possibly slightly better to use the $M = 1 \cdot 15$ nozzle with 24 minutes' convergence rather than the $M = 1 \cdot 0$ nozzle with the walls parallel.

The use of convergence to obtain off-design Mach numbers is therefore somewhat limited but it is probably fair to say that tests at smaller intervals in Mach number than $0 \cdot 05$ steps are not likely to be required in many cases for $M \geqslant 1 \cdot 15$.

The fact that use of convergence is not possible for $M \geqslant 1 \cdot 2$ is not of much significance in this context because it is already known that the perforated walls are reasonably effective in eliminating any serious reflection of a bow shock in front of a model for $M \geqslant 1 \cdot 2$. This can be taken as a very cautious statement and it will probably be found that it remains true down to some Mach number below $1 \cdot 2$.

6.4. *Position of the Fall-off in Mach Number at the Rear of the Working-Section at Supersonic speeds.* It has been mentioned previously that some interchange is possible between auxiliary suction and fan pressure ratio at a given M_{plenum} without changing the centre-line Mach-number distribution in the test region. On the other hand, it has been found that the position of the fall-off in Mach number at the rear of the working-section can be influenced by the fan pressure ratio used to obtain any given Mach number. This is particularly true for the highest test Mach numbers.

At supersonic speeds, the position of the terminal shock is probably the main factor determining the point at which the fall off begins; as the fan pressure ratio (at a given M_{plenum}) is increased, the terminal shock moves downstream and approaches the position that would be occupied by the bow wave in front of the model support strut. When this position is reached, one would expect that further increases of pressure ratio would have no significant effect on the position of the fall off.

The results plotted in Fig. 24 tend to support the concept just proposed. It should be noted that on this diagram, the fall-off position has been defined as the point at which the local centre-line Mach number is $0 \cdot 99$ M_{plenum}. The position of the fall-off moves downstream with increasing

Mach number between $M = 1 \cdot 0$ and $M = 1 \cdot 18$ but at higher Mach numbers, this trend is reversed. It can be concluded that $M = 1 \cdot 18$ probably corresponds to about the end of the range over which by suitable increase of fan pressure ratio the terminal shock can be made to coincide with or at least be determined by the strut bow-wave position. In other words, from $M = 1 \cdot 0$ to $M = 1 \cdot 18$, the fall-off moves downstream in sympathy with the approach of the strut bow wave towards the leading edge of the strut. At higher Mach numbers, however, the available fan pressure ratio is insufficient to hold the terminal shock back as far as this, and the margin by which it fails to do this increases with increasing Mach number. As a result, the terminal shock occurs further forward at the higher Mach numbers and from the point of view of where a model can be placed in the tunnel, $M = 1 \cdot 4$ is the most critical case at supersonic speeds.

It has been mentioned several times already that since the calibration has been completed, the model support strut has been moved about 8 in. downstream. The interpretation of Fig. 24 as given above would suggest that the fall-off position, for Mach numbers below $M = 1 \cdot 18$, may have moved downstream by a corresponding amount but that for Mach numbers greater than $1 \cdot 18$, the fall-off positions quoted on Fig. 24 probably still apply.

Fig. 24 shows that a representative position of the fall-off at $M = 1 \cdot 4$, is about station 120 in. The corresponding figure for $M = 1 \cdot 0$ is about 125 in. It would be expected that with a lifting model present in the working-section, the fall-off may occur further upstream and it would be wise to conclude that, for tests at supersonic speeds, the rear of a model should not be behind station 115 in. This position is, however, the rearmost limit beyond which the tunnel shock would probably interfere with the model tail or base; two typical sting diameters upstream of this point, at about 108 in. say, would be a better position to achieve if possible for the rear of a model. In any case, this is the recommended limit for tests at subsonic speeds (Section 4.3).

7. *The Validity of Plenum Pressure as an Indication of the Mean Mach Number in the Working-Section.* The plenum Mach number has been compared with the numerical average of the Mach numbers measured on the tunnel centre-line in the test region. This showed that with the perforated walls parallel, M_{plenum} is within $0 \cdot 002$ of the average Mach number with the trend being for M_{plenum} to be the higher value. Converging the walls gave a consistent measurable discrepancy. An average curve showing the observed differences is given in Fig. 25. According to this curve, there is an error of $0 \cdot 001$ in Mach number with the perforated walls parallel, increasing to $0 \cdot 008$ with 24 minutes' convergence. It is suggested that there is no need to apply a correction for this except when convergence of 12 minutes or more is being used.

8. *Power and Auxiliary-Suction Mass-Flow Requirements.* No very detailed systematic investigation into the power and auxiliary-suction requirements was made during the flow calibration. The complete readings necessary for the calculation of power consumption were only taken on a few occasions and Fig. 26 shows a plot from these readings. The values given refer to the tunnel empty with the perforated walls parallel. All the results have been reduced to a common stagnation pressure (30 in. Hg) and a stagnation temperature of 40 deg C and are expressed as motor shaft horse power per square foot of working-section area.

The curve 'total actual power' does not, however, give an entirely true picture because, as described in the introduction, due to the method of operating the compressor, the auxiliary-suction compressor power hardly varies with Mach number. This is because at the lower Mach numbers, when less auxiliary-suction mass flow is required by the tunnel, a correspondingly increased mass flow is allowed to circulate through the by-pass leg. Another curve labelled 'minimum possible total power' has therefore been added to indicate what the power requirements would have been if the auxiliary-suction compressor had been ideally matched to the mass-flow requirements of the tunnel at all Mach numbers (a compressor efficiency of $0 \cdot 8$ has been taken in these calculations). It should be noted, however, that to achieve this curve a compressor with both pressure ratio and volume flow separately variable would be required and it is unlikely this could be obtained in practice. Some saving in power could be obtained with a variable drive on the compressor.

It will be noted that the effect of the motor efficiencies has already been removed from the figures quoted but this would have only made a difference of the order of 3 per cent. It is considered that the final power values are encouragingly low.

The readings necessary for determining the auxiliary-suction mass flow were more readily accessible and these were noted throughout the calibration. The compressor circuit was calibrated at an early stage and the mass-flow quantities through the compressor and by-pass could therefore be deduced from measurements of the pressure at two points in the circuit, combined with the noted position of the by-pass valve. The results with the perforated walls parallel are summarised in Fig. 27. This graph is presented as a series of bands for each nozzle shape, the bands indicating the scatter in the experimental points. This scatter was largely due to the fact that no great care was taken to obtain any given Mach number with the same combination of fan pressure ratio and auxiliary-suction quantity on all occasions. Except with the $M = 1 \cdot 0$ nozzle, a considerable interchange between fan pressure ratio and auxiliary-suction quantity is possible with little effect on the centre-line Mach-number distributions. The tests with the $M = 1 \cdot 0$ nozzle were carried out at approximately constant fan pressure ratio and this is evidently why the scatter band in Fig. 26 is relatively narrower with this nozzle.

The cross-hatched band covers the condition for which the plenum Mach number was equal to that at the exit of the flow-forming nozzle. The results in Fig. 27 show clearly that use of these nozzles upstream of the working-section for $M \geqslant 1 \cdot 14$ has considerably reduced the auxiliary-suction requirements, *e.g.*, even for $M = 1 \cdot 14$, the required suction quantity is only about $1 \cdot 2$ per cent of the mass flow through the throat whereas if only the $M = 1 \cdot 0$ nozzle had been available, more than 2 per cent would have been required. (The curve in Fig. 27 suggests $1 \cdot 9$ per cent but it should be remembered that if there had only been the $M = 1 \cdot 0$ nozzle, a longer working-section with correspondingly greater auxiliary-suction requirements would have been needed.)

As the nozzle Mach number is increased, the variation of required mass flow with increasing plenum Mach number tends to increase. This is in accordance with two-dimensional-flow considerations.

Even allowing for the benefits due to the existence of the different nozzles, the suction quantities indicated in Fig. 27 are surprisingly low compared with the figures that have been quoted for various other tunnels. This is thought to be partly due to the relatively shorter working-section (about $1 \cdot 5 \times$ mean working-section height) and partly to a good choice of hole aspect ratio for the perforated walls (hole diameter/plate thickness $= 0 \cdot 5$ in./$0 \cdot 1875$ in.). In some other tunnels, the hole diameter/plate thickness has been nearer 1:1 and it is known that this would increase the auxiliary-suction requirements. Whatever the detailed reasons, the main experimental result is that a Mach number of $1 \cdot 4$ has been achieved with a flow removal of only about $1 \cdot 8$ per cent of the mass flow through the throat.

The results in Fig. 27 apply when the perforated walls are parallel. Some indication of the effect of converging the perforated walls on the auxiliary-suction mass-flow requirements is given in Fig. 28. The limited data for the $M = 1 \cdot 20$ nozzle were comparatively consistent and are therefore shown as a single curve. Fig. 28 shows that there is a rapid increase of auxiliary-suction flow required with increasing convergence. Converging by 36 minutes would approximately double the suction requirements.

Tests on a typical complete model have shown that the maximum available tunnel pressure ratio and auxiliary-suction mass flow are adequate to cope with a model set at an incidence giving a lift coefficient of about $0 \cdot 75$ at a Mach number of about $1 \cdot 4$ with a stagnation pressure of 1 Atm. It has proved impossible to lay down precise rules regarding what is the optimum combination of main-fan power and auxiliary-suction quantity for model tests because it has been found that relatively small changes in model configuration, *e.g.*, a change in the tail setting, can apparently have significant effects. The procedure generally adopted is to keep a check on the side-wall static-pressure distribution near the end of the perforated plate. If the terminal shock is observed to be tending to move upstream of about 6 in. forward of the end of the plate, this is usually an indication that the flow in the working-section is about to break down and that more fan pressure ratio is required to operate it at that particular Mach number.

9. *Conclusions and Recommendations for Further Work.* The following are the main conclusions and recommendations arising out of these tests:

9.1. *Centre-Line Mach-Number Distributions at Subsonic Speeds: Diffuser Suction only.*

(*a*) The maximum Mach number attainable with the perforated walls parallel was determined by choking of the flow around the model support strut at a Mach number in the working-section of about $1 \cdot 05$. Higher Mach numbers could be reached by diverging the perforated walls but the Mach-number distribution over the region that would be occupied by a typical model was unacceptable under these conditions. With a lifting model present in the working-section, Mach numbers in excess of $1 \cdot 00$ cannot be reached with diffuser suction only.

(*b*) In the test region, the centre-line Mach-number distribution is uniform to within $\Delta M = \pm 0 \cdot 002$ for all Mach numbers up to $1 \cdot 00$.

(*c*) The fall-off in Mach number at the rear of the working-section for Mach numbers near $0 \cdot 85$ dictates that the rear of a model should not be behind station 115 in. and if possible should be near or ahead of station 108 in., *i.e.*, about $0 \cdot 35 \times$ tunnel height ahead of the end of the perforated plate.

(*d*) To ensure that the fall off in Mach number is as far back as possible, the tunnel should be operated with the smallest possible diffuser-flap gap for any required Mach number.

9.2. *Centre-Line Mach-Number Distributions at Supersonic Speeds with Auxiliary Suction.*

9.2.1. $M = 1 \cdot 0$ *nozzle.*

(*a*) Modifications made to the open-area distribution on the side walls over the upstream part of the perforated plate were successful in attenuating an over-expansion found in the original centre-line Mach-number distributions for $M_{\text{plenum}} \geqslant 1 \cdot 07$ and in moving upstream the point beyond which the flow is reasonably uniform. The open-area distribution applying after the modification (Fig. 3b) is somewhat similar to what has been found to be necessary in tunnels with slotted walls.

(*b*) After the porosity modifications, for models about 6 ft long and having their nose somewhere near station 40 in., the Mach number should be uniform in the test region to within $\Delta M = \pm 0 \cdot 005$ for all Mach numbers up to about $1 \cdot 10$. With further increase in Mach number, there is a deterioration to $\pm 0 \cdot 011$ at $M = 1 \cdot 12$. If the model does not extend forward of station 50 in., the favourable Mach number range is extended and the scatter for $M = 1 \cdot 12$ is then reduced to $\Delta M = \pm 0 \cdot 007$.

(*c*) Another way of expressing conclusion (*b*) above is that at $M = 1 \cdot 095$, a distance of only about $0 \cdot 4 \times$ tunnel height is required downstream of the start of the perforated plate on the side walls for a uniform flow to become established. This compares very favourably with experience elsewhere and shows the benefits that have been produced by the refinements to the upstream open-area distributions.

(*d*) Converging the side perforated walls reduces any tendency for an over-expansion to occur but moves the point of flow establishment further downstream. As a result, convergence by more than 6 minutes is not possible for Mach numbers greater than $1 \cdot 06$ unless a very short model is being tested.

(*e*) It is thought that further improvements in the centre-line Mach-number distributions for Mach numbers above $1 \cdot 10$, walls parallel, could be obtained by further changes to the open-area distributions on both the side walls (curve D, Fig. 3b) and preferably, the floor and ceiling as well.

(*f*) If reflected shock-wave-attenuation considerations ultimately require the perforated walls to be converged at these Mach numbers, fairly radical changes to the open-area distribution at the upstream end of the perforated plates will be necessary.

9.2.2. *Supersonic nozzles.*

(*a*) The centre-line Mach-number distributions obtained with the $M = 1 \cdot 15$, $1 \cdot 20$, etc., nozzles are very sensitive to whether the value of M_{plenum} corresponds to the Mach number at the exit of the nozzle. If the side perforated walls are set parallel, the best distributions were obtained when these two Mach numbers were equal but if the walls were converged, it was preferable to run the tunnel at Mach numbers that could be as much as $0 \cdot 02$ higher than the minimum possible with the given nozzle and perforated wall settings.

(*b*) With the $M = 1 \cdot 15$ nozzle, the best distribution was obtained with the side walls converged by 6 minutes. This had the effect of removing a small positive gradient present through the rear part of the working-section if the walls were set parallel. At higher Mach numbers, the best distributions were obtained with the walls parallel. The following Table gives the Mach-number scatter bands* for the test region at the recommended perforated-wall settings and plenum Mach numbers.

* The values quoted may err on the conservative side because they include tube and other measuring errors.

Nozzle.	1·15	1·20	1·25	1·30	1·35	1·40
Wall Setting.	6 min converged	Parallel	Parallel	Parallel	Parallel	Parallel
M_{plenum}	1·15	1·19	1·245	1·30	1·35	1·395
$\pm\ \Delta M$	0·006	0·0075	0·010	0·011	0·012	0·016

These values refer to a test region of about 6 ft long.

(*c*) The deterioration in the standard of flow uniformity with increasing Mach number is largely due to disturbances originating from changes in slope near the saw-teeth junction between the nozzle and perforated floor. These disturbances cross the centre-line near a typical model nose position at the lower supersonic Mach numbers but for $M = 1 \cdot 4$, their effect extends to downstream of the model centre of rotation. Some reduction in the scatter band widths at the higher Mach numbers might therefore be achieved by improving the fit of the floor at the upstream end. If the model tested is relatively short, it can be placed in the rear part of the working-section so that its nose is behind these particular disturbances even at the highest Mach number. In such cases, ΔM would be less than $\pm\ 0 \cdot 007$ even at $M = 1 \cdot 40$. It is important to note that this is the figure that should be compared with the values quoted for various other tunnels which have a longer working-section and where a model is never placed upstream of any disturbances originating from the start of the working-section.

(*d*) Converging the side perforated walls by more than 6 minutes results in a deterioration of the flow uniformity and is probably only acceptable with the $M = 1 \cdot 15$ nozzle. To operate at $M = 1 \cdot 12$, use of the $1 \cdot 15$ nozzle with 24 minutes' convergence gives a distribution comparable with that obtained with the $M = 1 \cdot 0$ nozzle, walls parallel.

(*e*) For Mach numbers up to $1 \cdot 15$, the fan pressure ratio is sufficient to pull the terminal shock back to a position determined by the bow wave in front of the model support strut but with increasing Mach number beyond $M = 1 \cdot 15$, the terminal shock moves forward owing to insufficient fan pressure ratio. As for tests at subsonic speeds, it is recommended that the tail of a model should not be aft of station 115 in. and should if possible be near or ahead of station 108 in., *i.e.*, about $0 \cdot 35h \sim 0 \cdot 4h$ upstream of the end of the perforated plate.

9.3. *Use of Plenum Pressure as an Indication of the Mean Mach Number in the Working-Section.* If the side perforated wall is not converged by more than 5 minutes, the difference between the arithmetic mean of the measured centre-line Mach numbers over the test region and the value of M_{plenum} (tunnel empty) is trivial. As the convergence is increased, some correction to M_{plenum} becomes necessary, *e.g.*, a correction of $-\ 0 \cdot 008$ in Mach number for 24 minutes' convergence.

9.4. *Tunnel Power Requirements.* A Mach number of $1 \cdot 40$ can be achieved at atmospheric stagnation pressure with the tunnel empty for a total power consumption of 440 h.p./sq ft of working-section area. This figure can be reduced to 380 h.p./sq ft if the auxiliary-compressor mass flow were accurately matched to the auxiliary-suction requirements of the tunnel at this Mach number. Tests on a typical complete model have shown that there is sufficient reserve of power to cope with a model set at an incidence giving $C_L = 0 \cdot 75$ at $M = 1 \cdot 4$, atmospheric stagnation pressure.

9.5. *Auxiliary-Suction Requirements.* With the side perforated walls parallel, a Mach number of $1 \cdot 4$ is achieved with a flow removal of only about $1 \cdot 8$ per cent of the mass flow through the throat. For $M = 1 \cdot 14$, the corresponding value is $1 \cdot 2$ per cent if the $M = 1 \cdot 15$ nozzle is used compared with about 2 per cent if the $M = 1 \cdot 0$ nozzle were used. These remarkably small suction requirements are due to the use of the flexible nozzle ahead of the working-section, to the relatively short working-section ($1 \cdot 52h$) and to a good choice of hole aspect ratio. Converging the side perforated walls results in a considerable increase in the suction requirements, *e.g.*, converging by 36 minutes for $M = 1 \cdot 2$ would approximately double them.

LIST OF SYMBOLS

M_{plenum}	Mach number derived from the static pressure measured at a tapping in the top of the pressure shell surrounding the plenum chamber and the total-head pressure in the working-section which is known to agree closely with the static pressure measured at a tapping in the settling chamber
M_M	The average centre-line Mach number over the region occupied by a typical model
M_{nozzle}	The Mach number generated at the exit of the nozzle
ΔM	Scatter band derived from the centre-line Mach-number distribution over the test region
$\Delta \bar{M}$	The average of the values of ΔM obtained from the upper and lower tappings on the centre-line static tube
h	Test-section height

APPENDIX

The Design of the Flexible Nozzle

The nozzle shapes for the A.R.A. Transonic Wind Tunnel were worked out by characteristics using a parabolic wall shape at the sonic throat and the Sauer theory. The ordinates of the nozzles were obtained by integrating the slopes. A boundary-layer correction amounting to 0·004 in. was applied to the upper wall only.

The shape of the contraction ahead of the throat was a 1/6th order polynomial. The slope and ordinate at the start of the contraction (station − 280) and the radius of curvature, slope and ordinate at the nozzle throat were specified to find the constants of the polynomial.

The following Tables give the ordinates of the upper and lower walls with respect to the centre-line of the tunnel. The jack positions are referred to the datum at the start of the perforated plate on the side walls. With respect to this datum, the nozzle ends at + 20 in. Because of the boundary-layer correction, the ordinates for the upper wall are not quite the same; at the end of the nozzle, y = 47·4 in. for the upper wall as compared with 48·0 in. for the lower wall.

ORDINATES OF LOWER FLEXIBLE NOZZLE FROM CENTRE-LINE OF TUNNEL

Distances Measured from Start of Vertical Perforated Wall Negative Upstream

Jack position	y in.						
	M = 1·0	M = 1·15	M = 1·2	M = 1·25	M = 1·3	M = 1·35	M = 1·4
+ 20	48·000	48·000	48·000	48·000	48·000	48·000	48·000
− 10	48·000	47·994	47·977	47·964	47·940	47·926	47·911
− 23·5	48·000	47·965	47·916	47·880	47·819	47·777	47·740
− 37	48·000	47·891	47·791	47·723	47·601	47·513	47·434
− 50·5	48·000	47·760	47·588	47·474	47·266	47·106	46·966
− 64	48·000	47·578	47·314	47·135	46·813	46·555	46·329
− 77·5	48·000	47·383	47·014	46·737	46·285	45·888	45·553
− 91	48·000	47·235	46·754	46·344	45·742	45·187	44·703
− 104·5	48·012	47·186	46·616	46·041	45·294	44·557	43·874
− 118	48·167	47·237	46·616	45·895	45·071	44·185	43·285
− 131·5	48·475	47·408	46·760	45·911	45·094	44·150	43·117
− 145	48·962	47·746	47·078	46·105	45·375	44·454	43·383
− 158·5	49·669	48·308	47·617	46·534	45·944	45·106	44·081
− 172	50·616	49·147	48·427	47·275	46·838	46·118	45·198
− 185·5	51·803	50·303	49·552	48·398	48·094	47·499	46·717
− 199	53·239	51·796	51·021	49·947	49·733	49·251	48·615
− 212·5	54·906	53·618	52·844	51·926	51·754	51·361	50·866
− 226	56·793	55·739	55·005	54·299	54·134	53·816	53·438
− 239·5	58·890	58·106	57·467	56·993	56·823	56·567	56·292
− 253	61·156	60·653	60·171	59·907	59·752	59·564	59·381
− 266·5	63·553	63·305	63·044	62·937	62·839	62·736	62·642
− 280	66·000	66·000	66·000	66·000	66·000	66·000	66·000
Throat position	− 80	− 104·5	− 111·25	− 123·34	− 123·5	− 126·2	− 130
Throat height	48·000	47·186	46·599	45·882	45·050	44·124	43·114

ORDINATES OF UPPER FLEXIBLE NOZZLE FROM CENTRE-LINE OF TUNNEL

Distances Measured from Start of Vertical Perforated Wall Negative Upstream

Jack position	*y* in.						
	$M = 1\cdot0$	$M = 1\cdot5$	$M = 1\cdot2$	$M = 1\cdot25$	$M = 1\cdot3$	$M = 1\cdot35$	$M = 1\cdot4$
+ 20	47·400	47·400	47·400	47·400	47·400	47·400	47·400
− 10	47·280	47·274	47·257	47·245	47·224	47·205	47·191
− 23·5	47·226	47·191	47·142	47·107	47·049	47·003	46·966
− 37	47·172	47·063	46·963	46·895	46·777	46·685	46·606
− 50·5	47·118	46·878	46·706	46·593	46·388	46·224	46·084
− 64	47·064	46·642	46·378	46·199	45·881	45·619	45·393
− 77·5	47·010	46·393	46·024	45·747	45·299	44·898	44·563
− 91	47·025	46·191	45·710	45·301	44·702	44·143	43·659
− 104·5	47·148	46·088	45·518	44·943	44·200	43·459	42·776
− 118	47·373	46·085	45·464	44·743	43·923	43·033	42·133
− 131·5	47·745	46·212	45·558	44·706	43·892	42·944	41·911
− 145	48·298	46·530	45·845	44·852	44·126	43·198	42·125
− 158·5	49·071	47·115	46·391	45·261	44·674	43·824	42·790
− 172	50·084	48·032	47·264	46·034	45·601	44·817	43·920
− 185·5	51·337	49·322	48·514	47·258	46·957	46·336	45·522
− 199	52·841	50·995	50·164	48·978	48·766	48·256	47·583
− 212·5	54·574	53·027	52·202	51·183	51·013	50·585	50·062
− 226	56·527	55·358	54·587	53·804	53·639	53·301	52·894
− 239·5	58·690	57·907	57·246	56·725	56·555	56·287	55·995
− 253	61·024	60·580	60·090	59·807	59·652	59·459	59·268
− 266·5	63·487	63·294	63·031	62·921	62·823	62·719	62·625
− 280	66·000	66·000	66·000	66·000	66·000	66·000	66·000
Throat position	− 80	− 104·5	− 111·25	− 123·34	− 123·5	− 126·2	− 130·0
Throat height	47·000	46·088	45·474	44·709	43·880	42·939	41·914

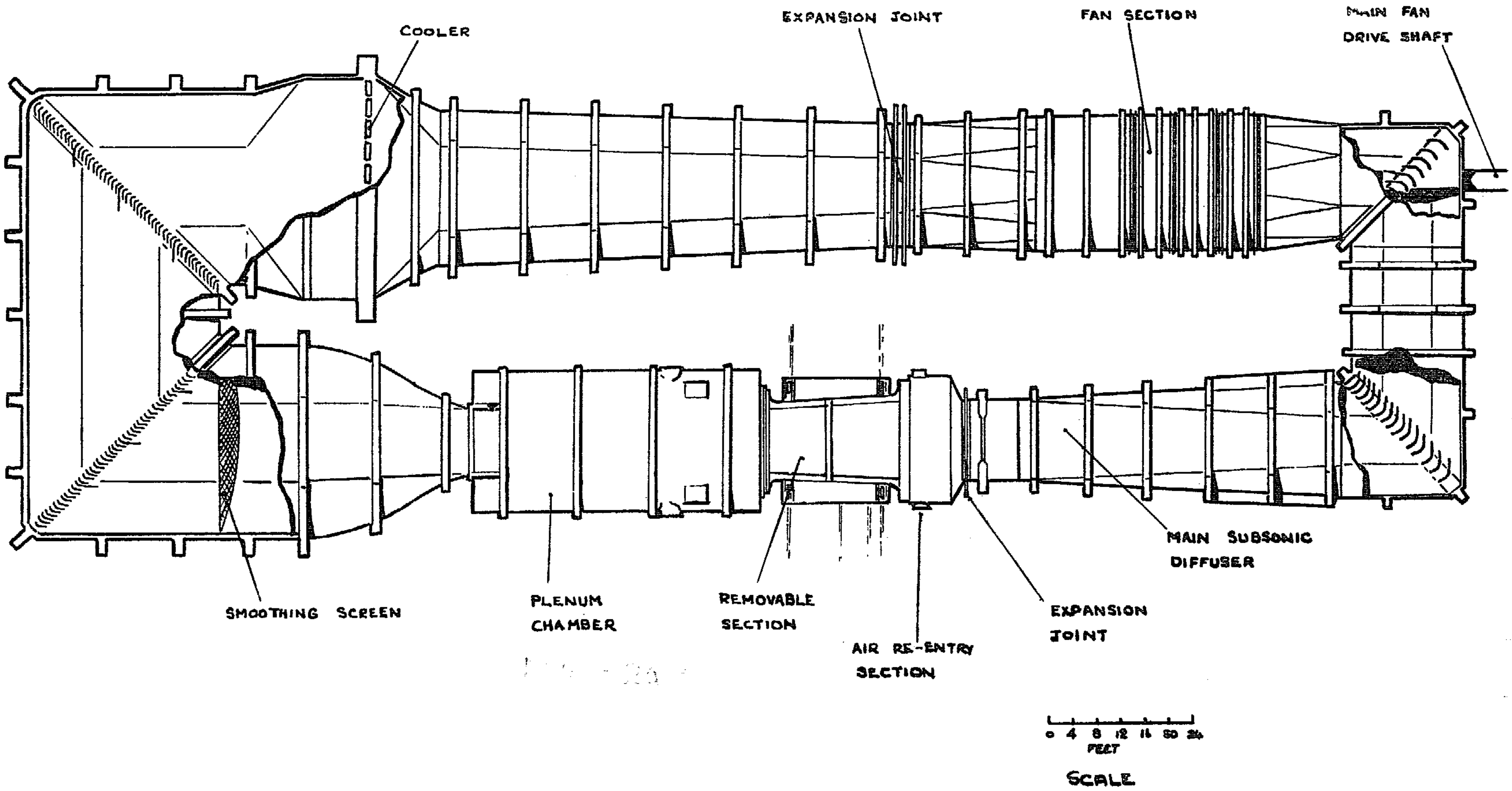

FIG. 1. Tunnel circuit.

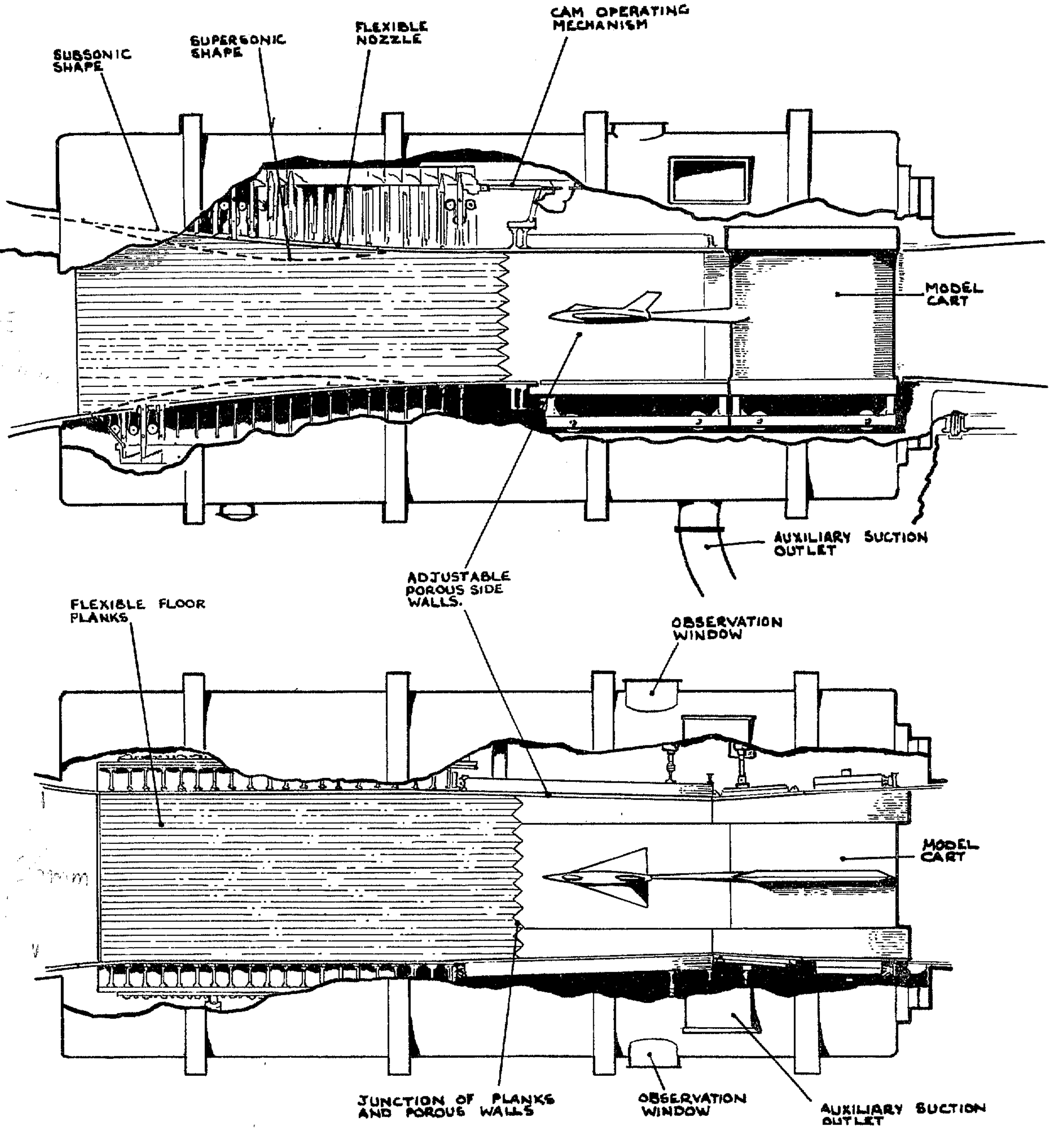

FIG. 2a. Working-section and plenum chamber.

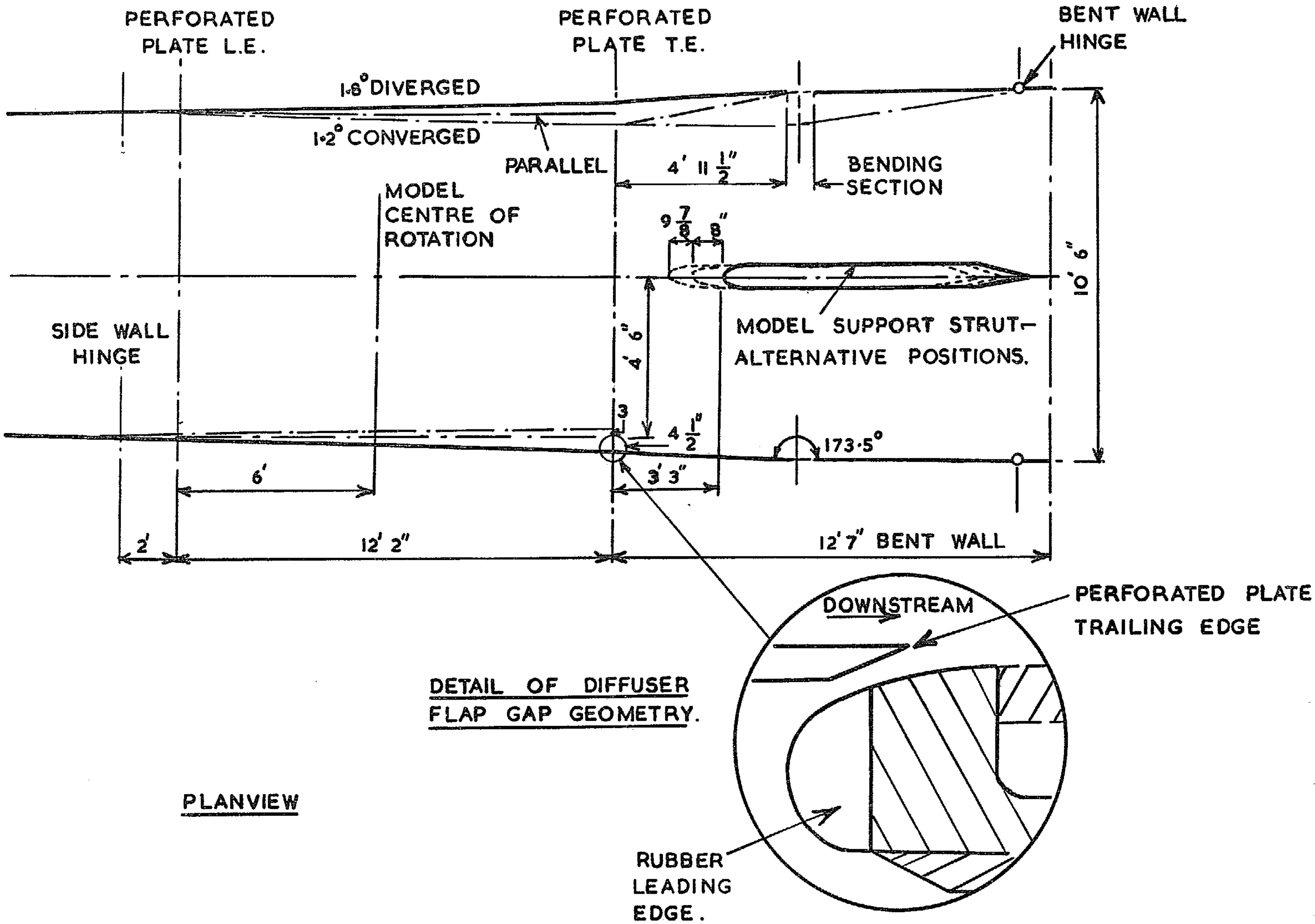

FIG. 2b. Salient features of working-section and bent-wall geometry.

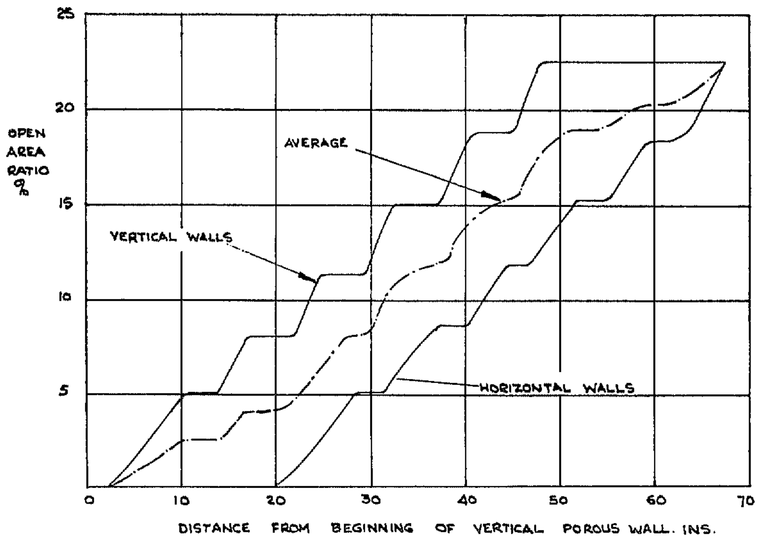

FIG. 3a. Perforated-wall porosity distribution—Original porosity.

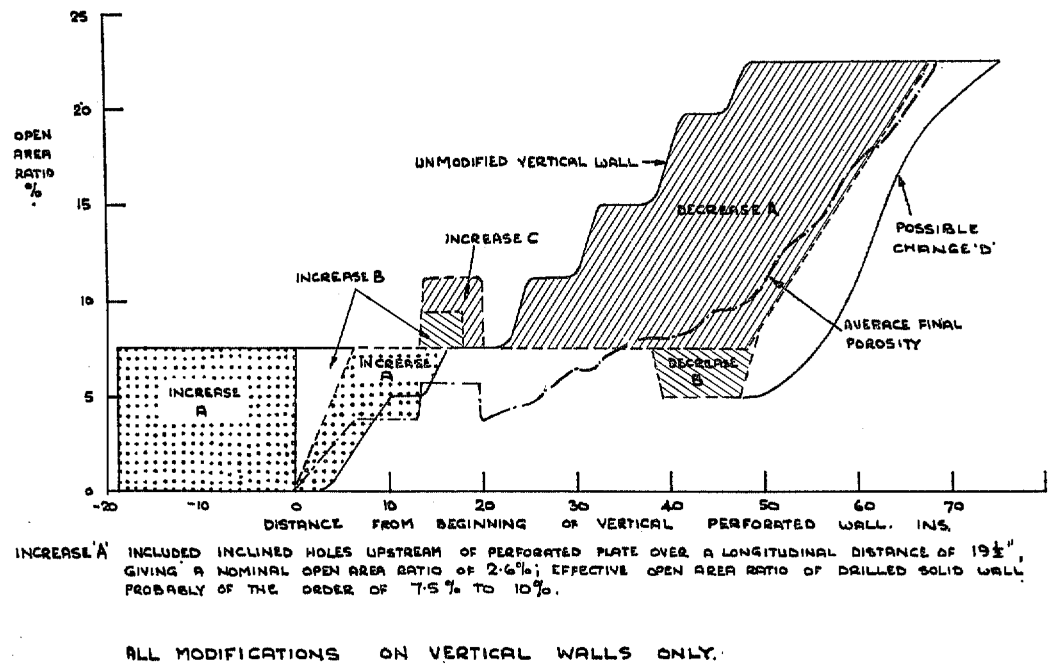

FIG. 3b. Perforated-wall porosity distribution—Modified porosity. Final perforated wall has all modifications shown except decrease B.

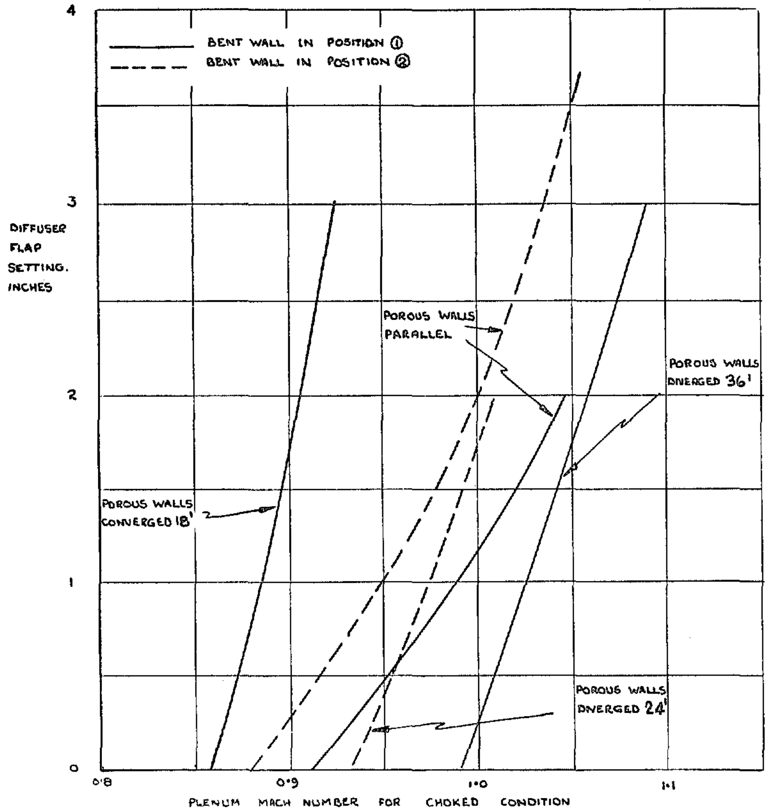

NO AUXILIARY SUCTION

FIG. 4. Variation of maximum attainable Mach number with diffuser flap opening.

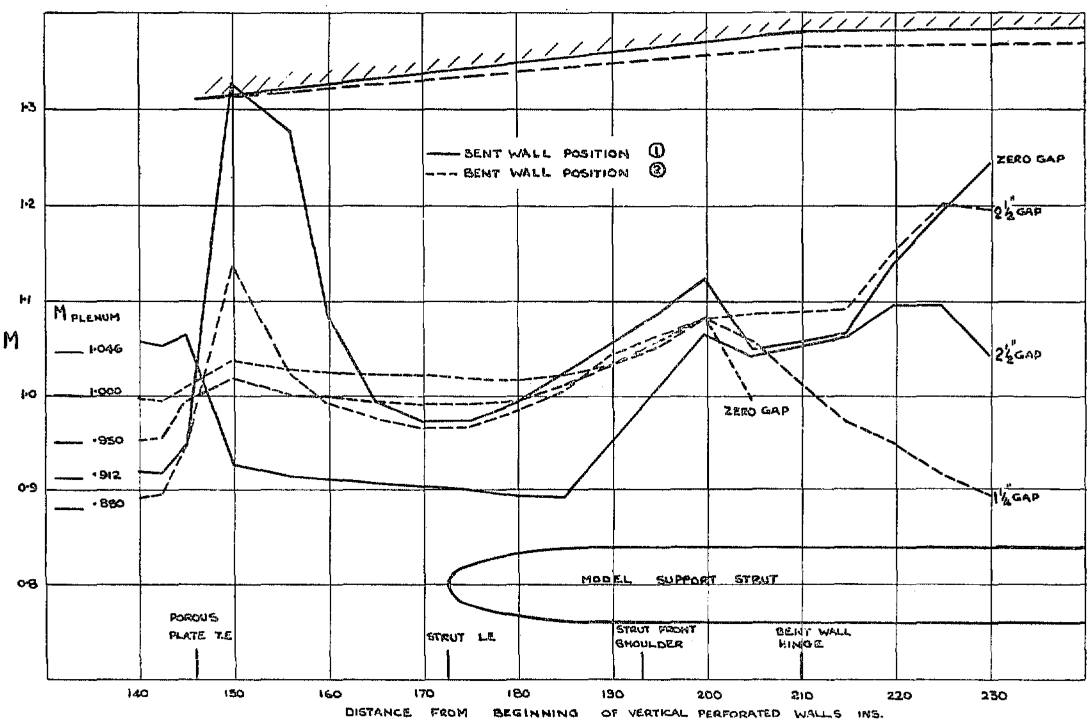

FIG. 5. Mach-number distribution along bent wall.—Perforated walls parallel; various flap gaps.

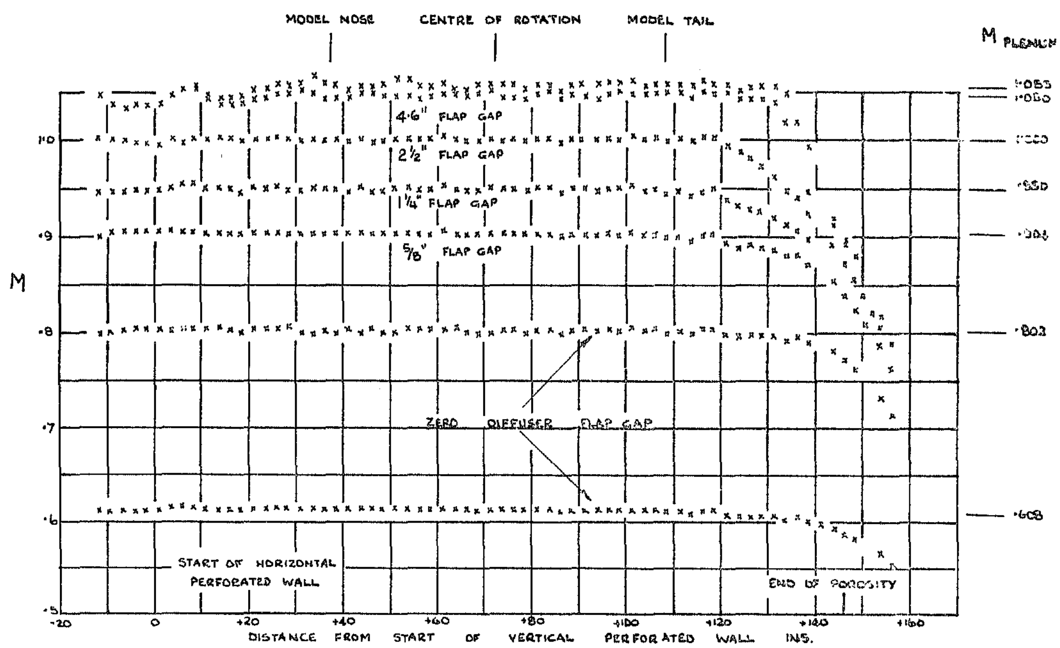

FIG. 6. Centre-line Mach-number distribution for recommended gap sizes—Diffuser suction only.

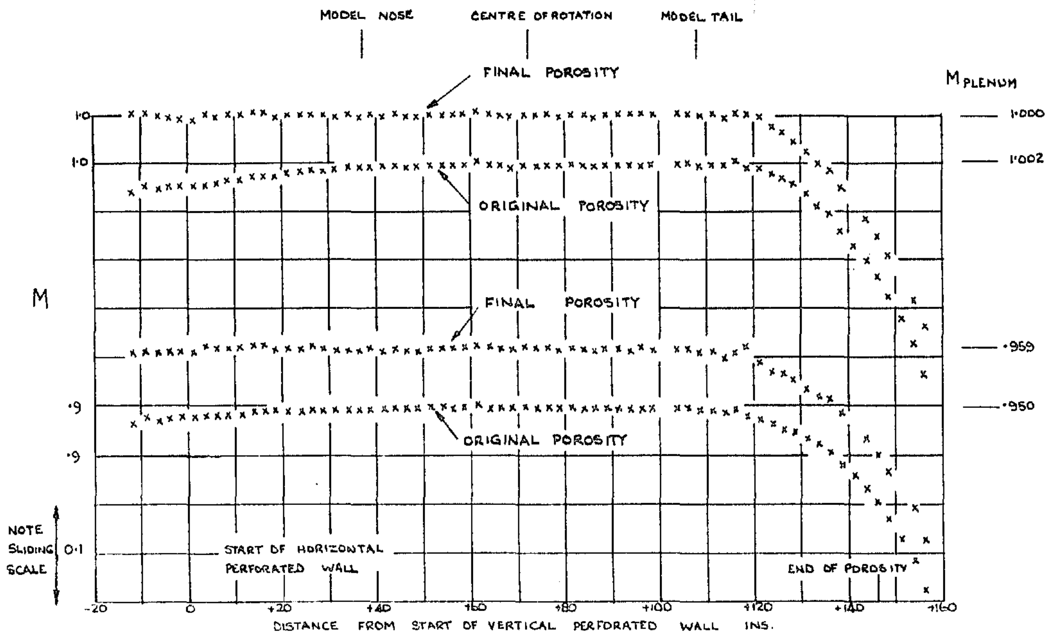

FIG. 7. Effect of main porosity modifications on centre-line Mach-number distribution with diffuser suction only.

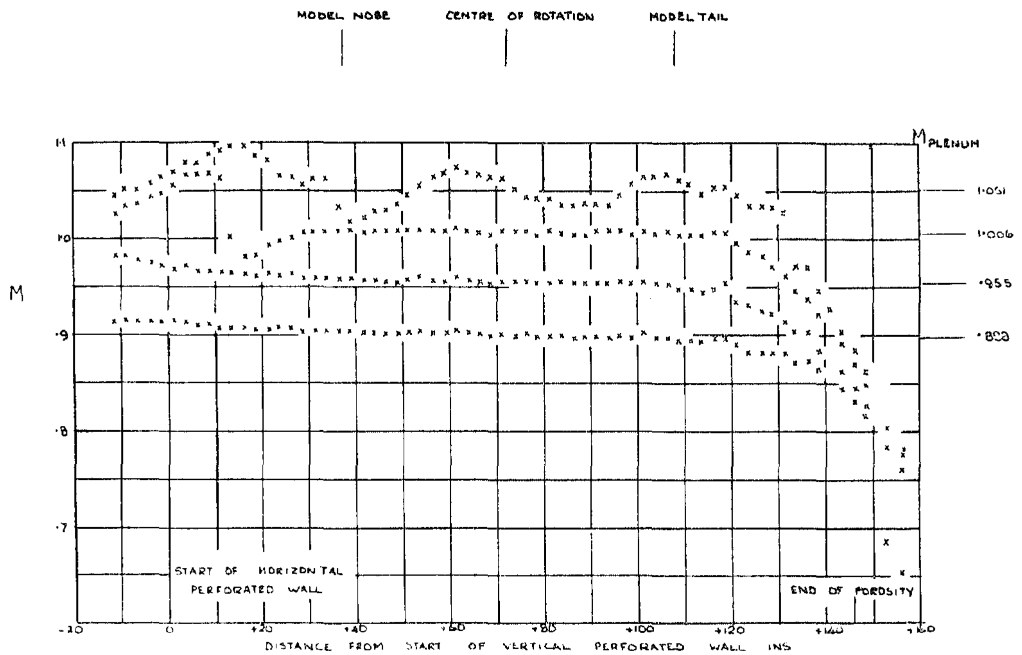

FIG. 8. Centre-line Mach-number distribution.—Walls diverged 24 minutes; diffuser suction only.

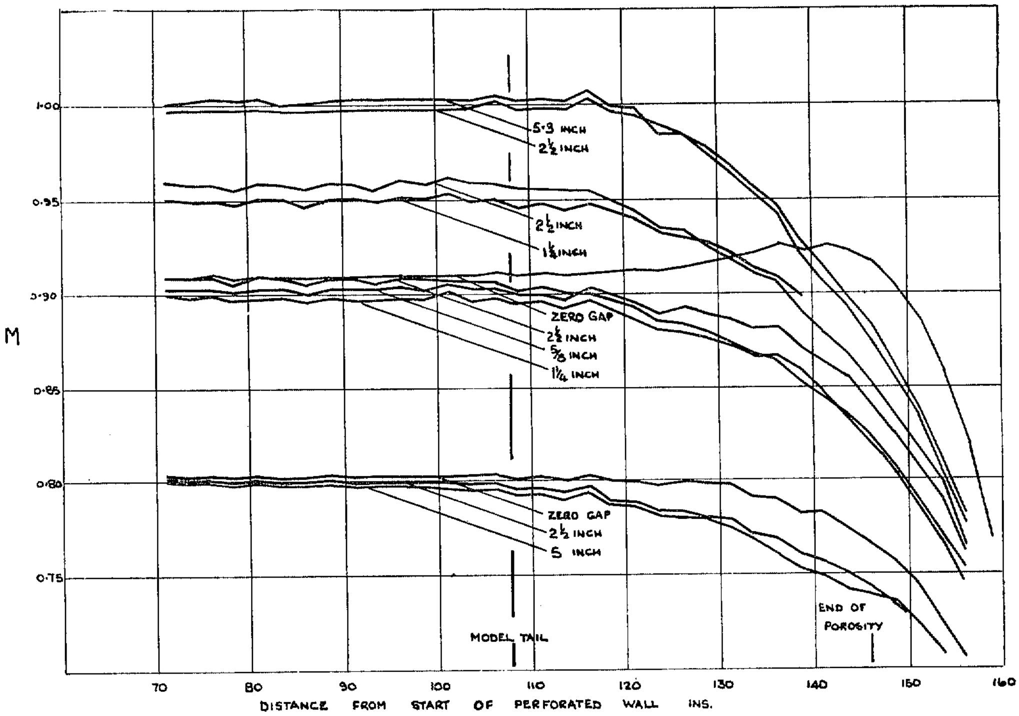

FIG. 9. Effect of diffuser-flap opening on the downstream centre-line Mach-number distribution.—Perforated walls parallel.

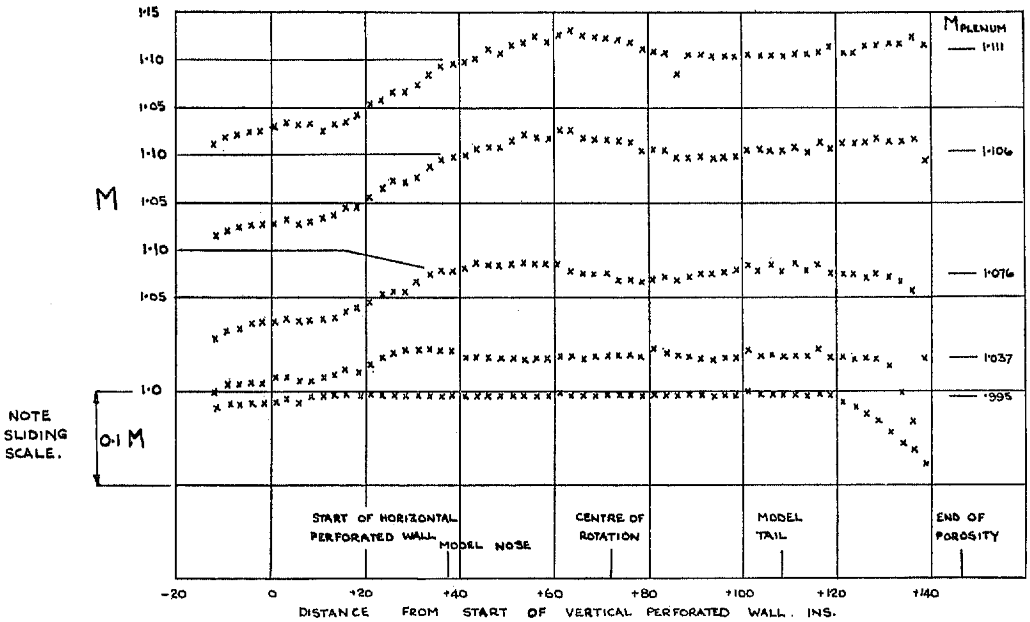

FIG. 10. $M = 1 \cdot 0$ nozzle. Perforated walls parallel. Auxiliary suction.—Centre-line Mach-number distributions before porosity modifications.

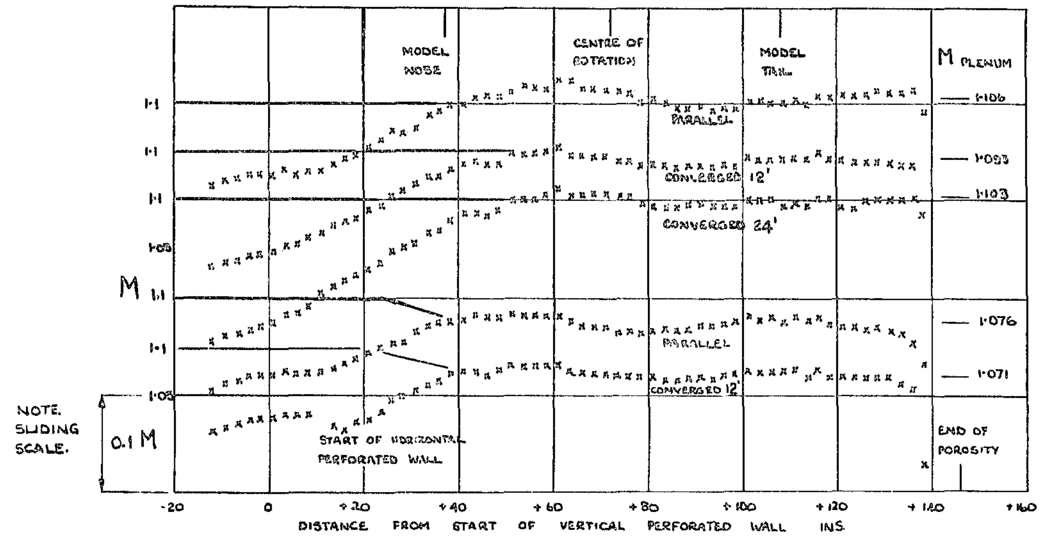

FIG. 11. Centre-line Mach-number distribution before porosity modification.—Effect of wall convergence.

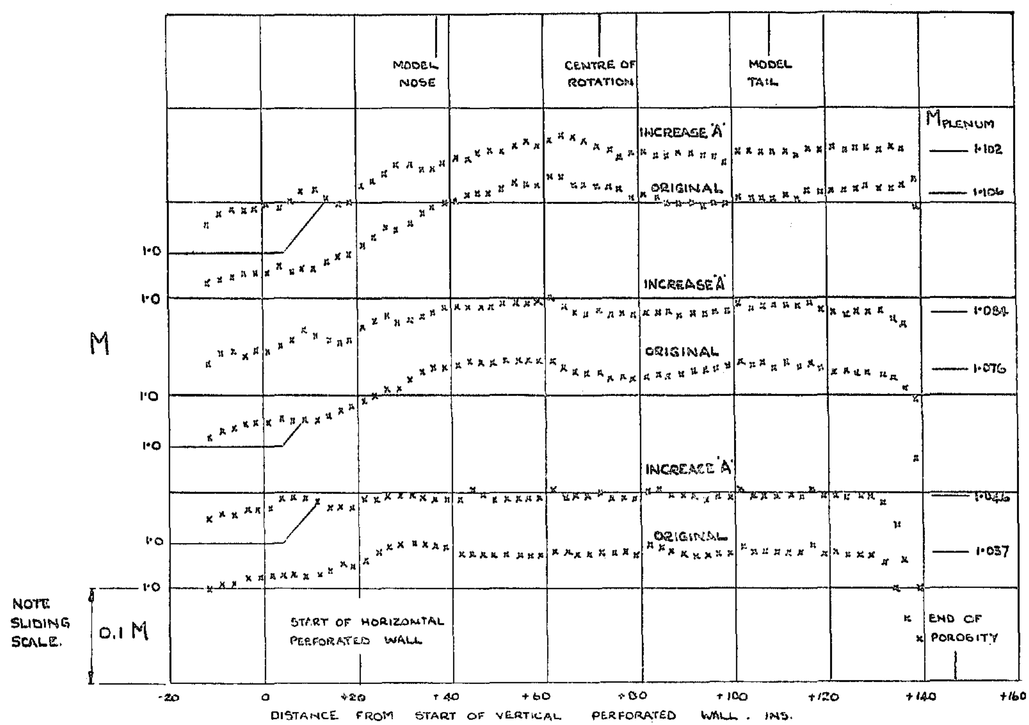

FIG. 12. Centre-line Mach-number distributions.—Effect of porosity increase A (Stage 1 modification).

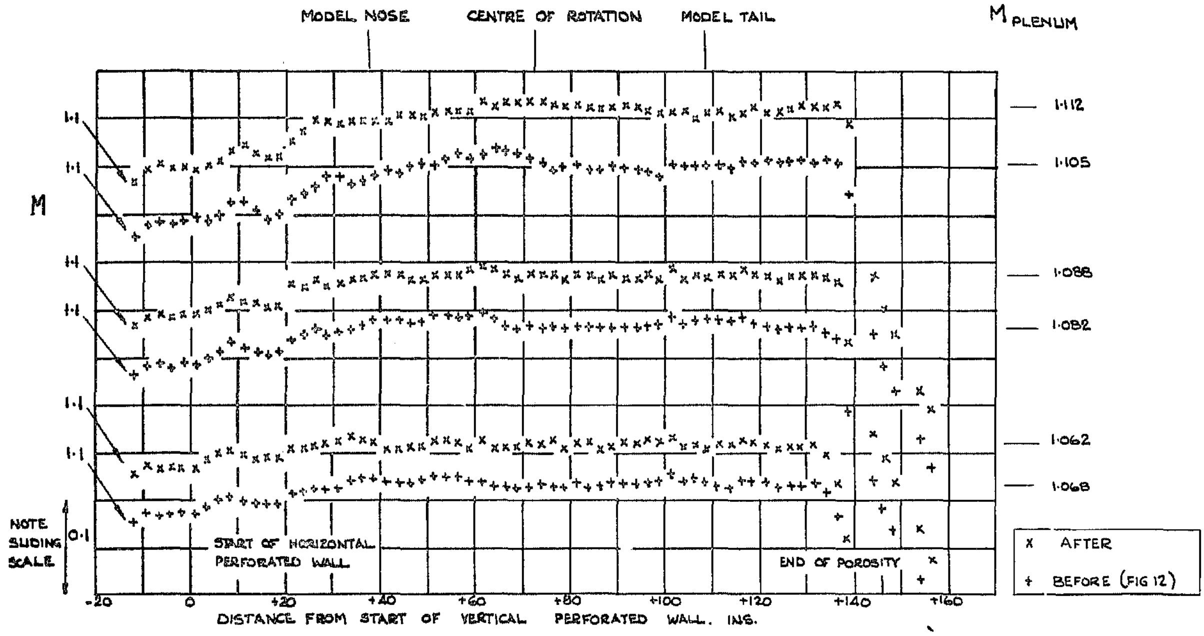

FIG. 13. Effect of decrease A + increase B on centre-line Mach-number distribution at $M \approx 1 \cdot 06$, $1 \cdot 08$ and $1 \cdot 10$.

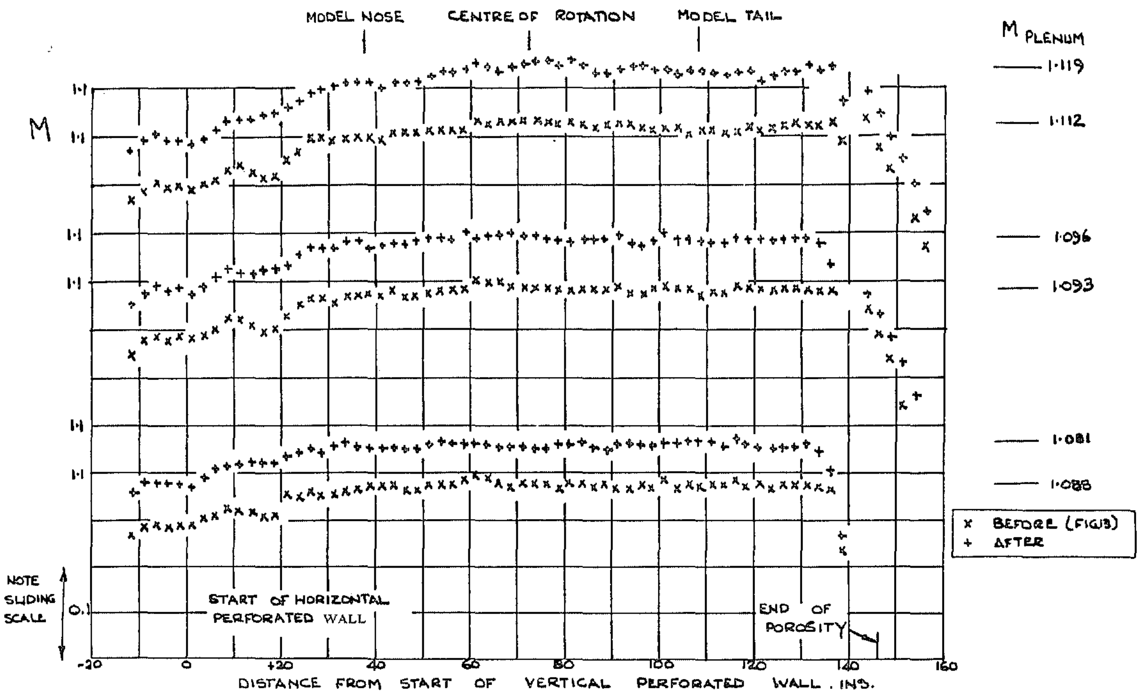

FIG. 14. Effect of increase C on centre-line Mach-number distribution at $M \approx 1 \cdot 08$, $1 \cdot 10$ and $1 \cdot 12$.

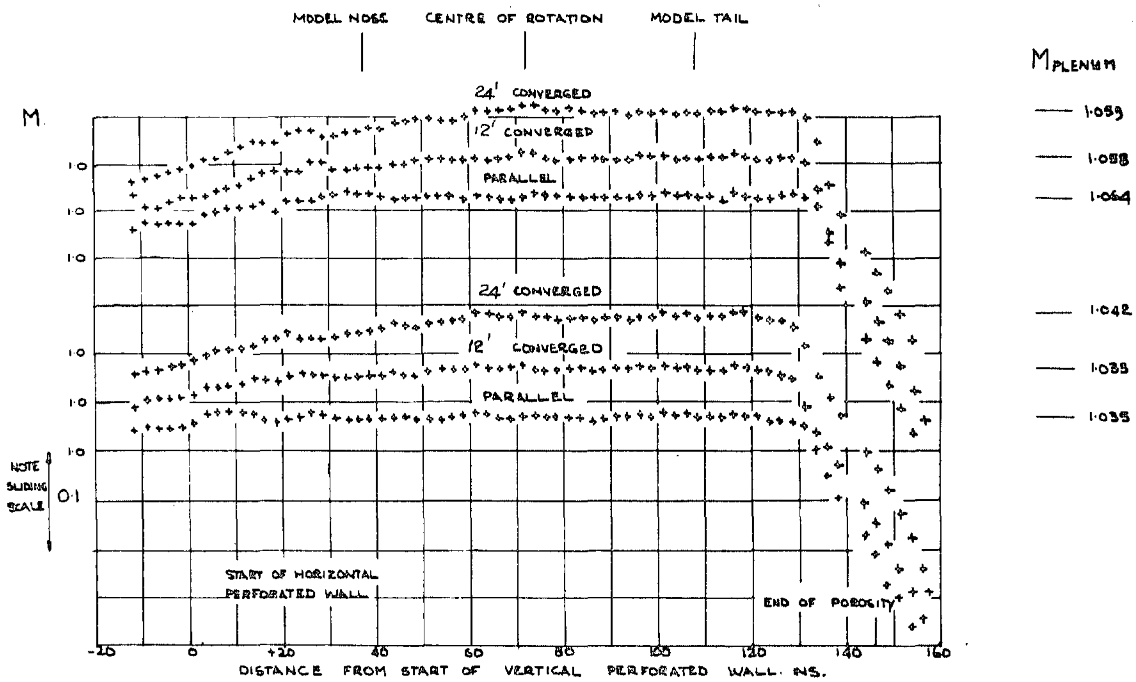

FIG. 15a. Effect of perforated-wall convergence on centre-line Mach-number distribution.—Final porosity distribution. $M \approx 1\cdot04$ and $1\cdot06$.

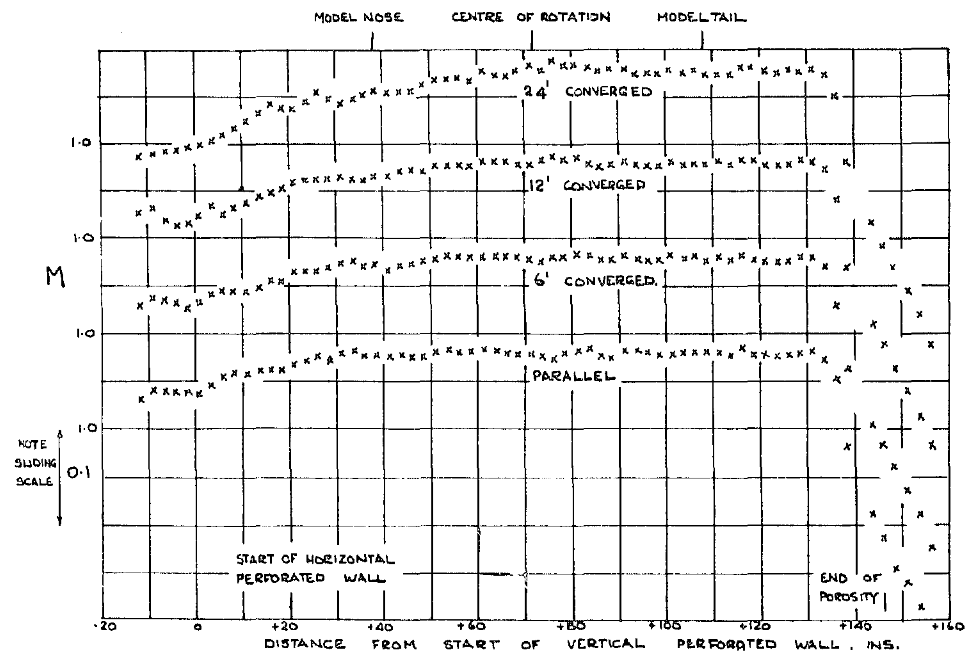

FIG. 15b. Effect of perforated-wall convergence on centre-line Mach-number distribution.—Final porosity distribution. $M \approx 1\cdot08$.

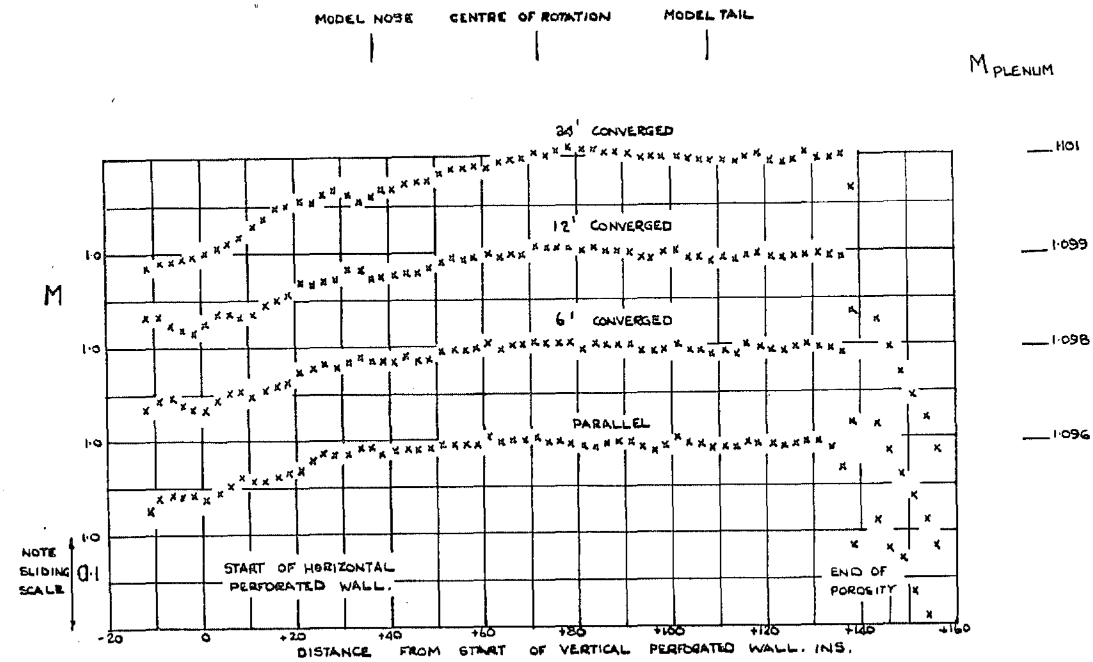

FIG. 15c. Effect of perforated-wall convergence on centre-line Mach-number distribution.—Final porosity distribution. $M \approx 1 \cdot 10$.

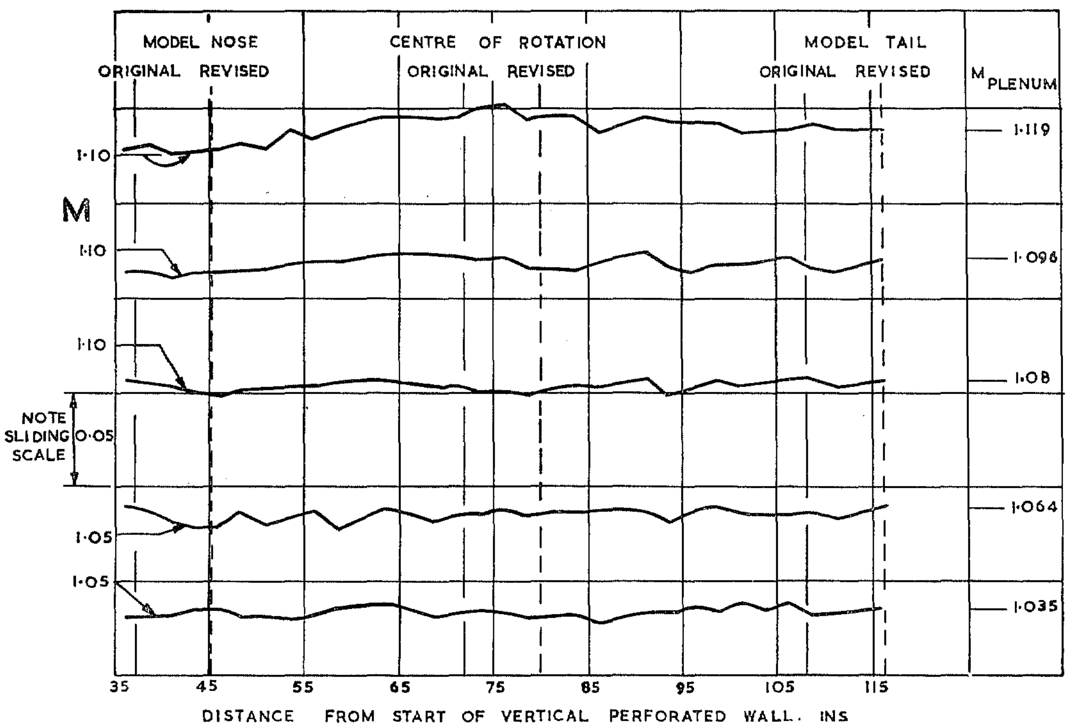

FIG. 16a. Centre-line Mach-number distribution in region of model with porous wall in final condition.—Walls parallel.

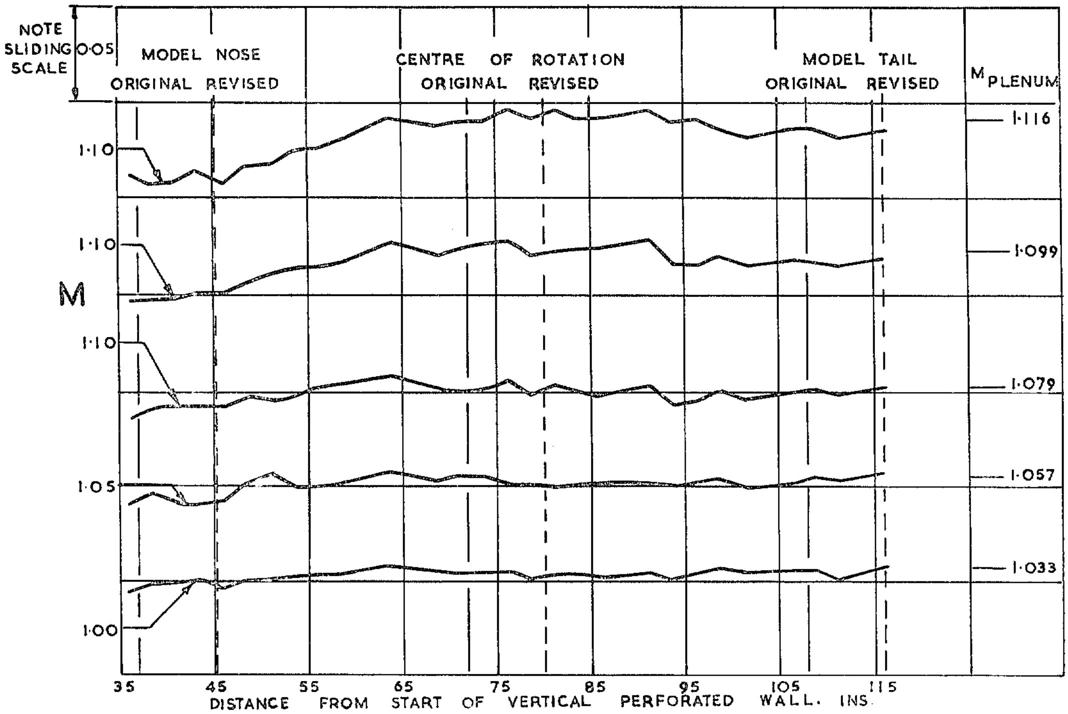

FIG. 16b. Centre-line Mach-number distribution in region of model with porous wall in final condition.—Walls 12 minutes converged.

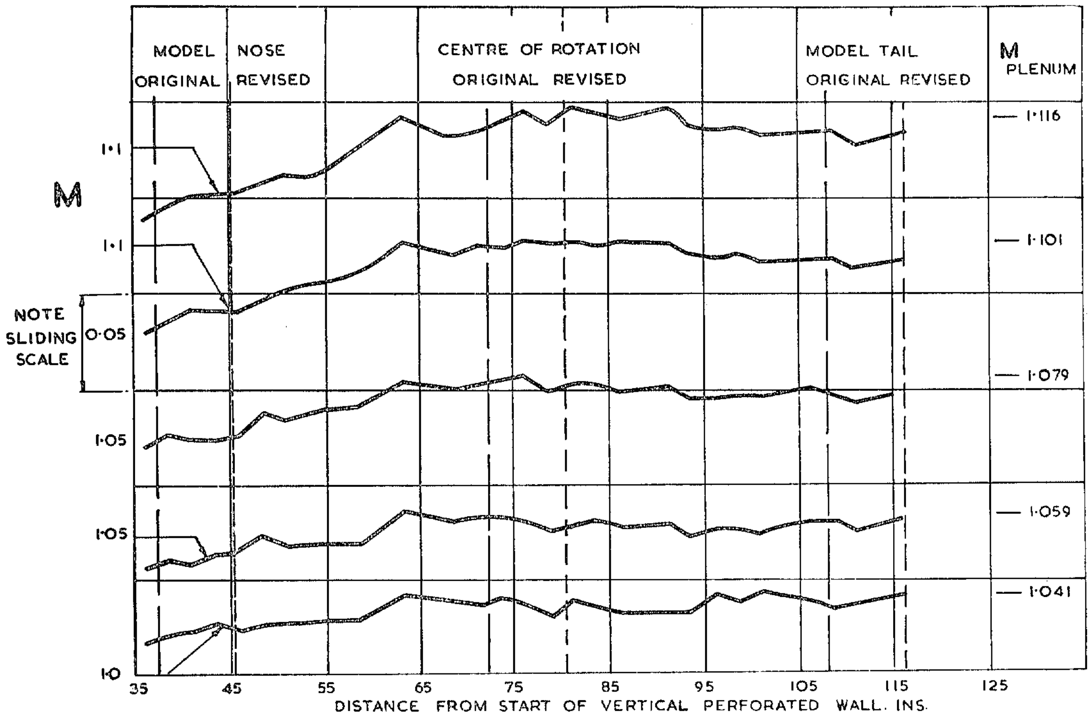

FIG. 16c. Centre-line Mach-number distribution in region of model with porous wall in final condition.—Walls 24 minutes converged.

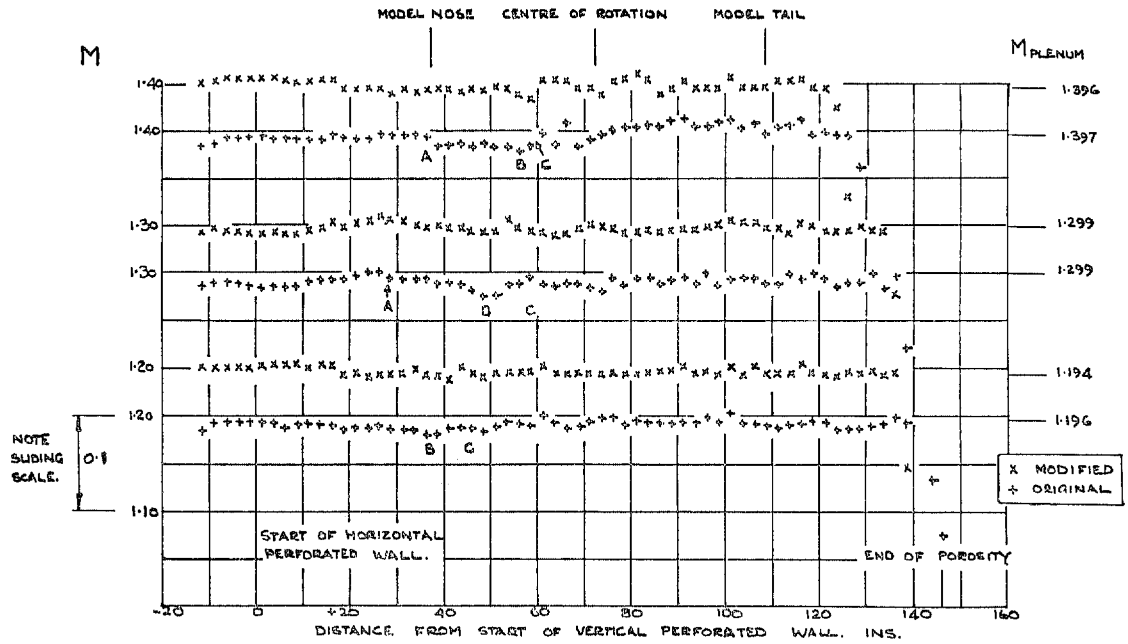

FIG. 17. Effect of realignments and porosity modification on design Mach-number distribution.

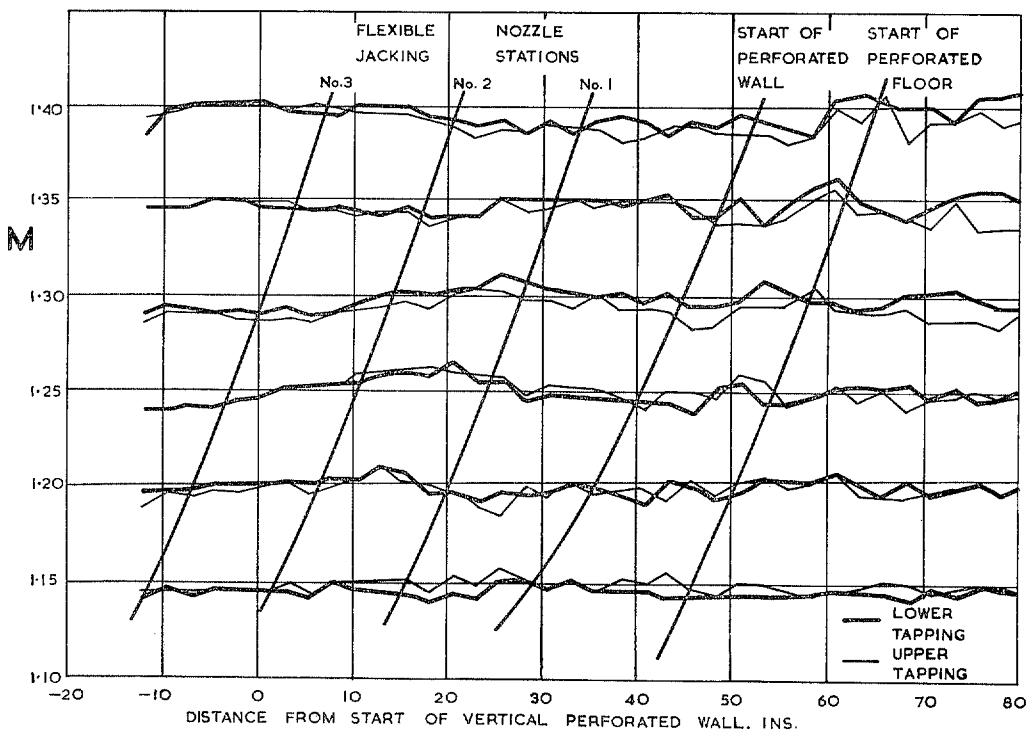

FIG. 18. Mach-number distributions $2\frac{1}{4}$ in. above and below the centre-line.—Perforated walls parallel. Wall modifications partially completed.

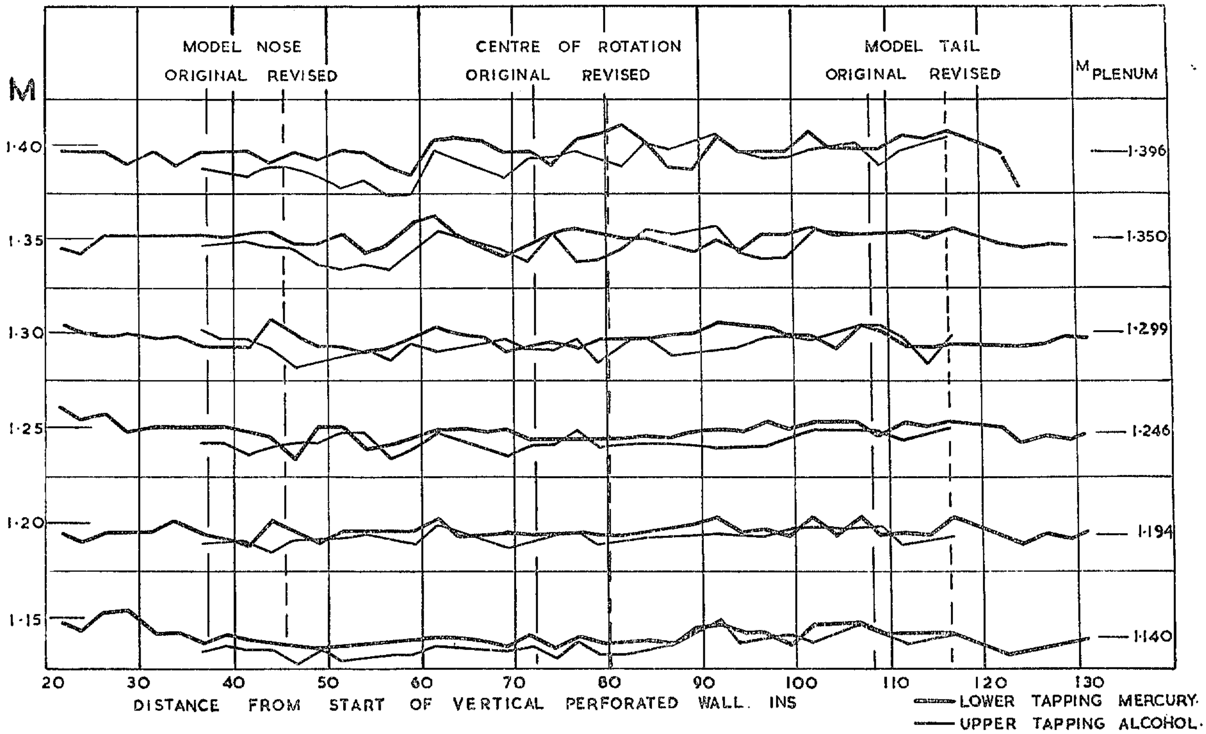

FIG. 19. Centre-line Mach-number distribution at the flexible nozzle design Mach numbers.—Perforated walls parallel.

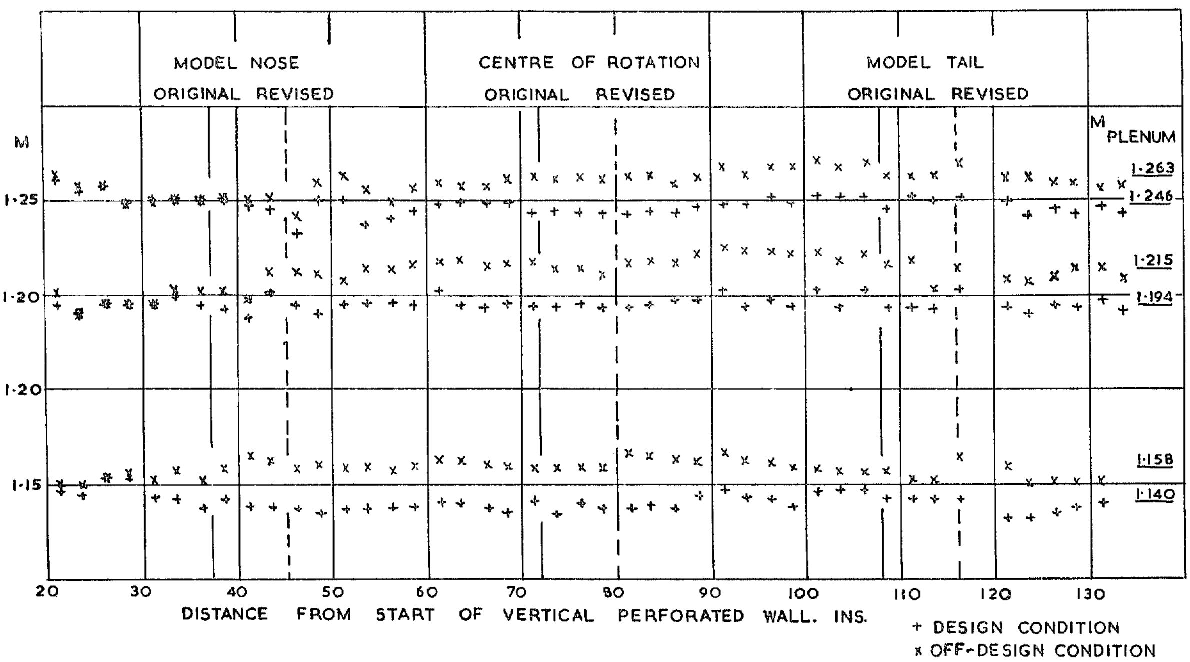

FIG. 20. Comparison of the centre-line Mach-number distributions at design and off-design Mach numbers.—Perforated walls parallel; $M = 1\cdot15$, $1\cdot20$ and $1\cdot25$ nozzle settings.

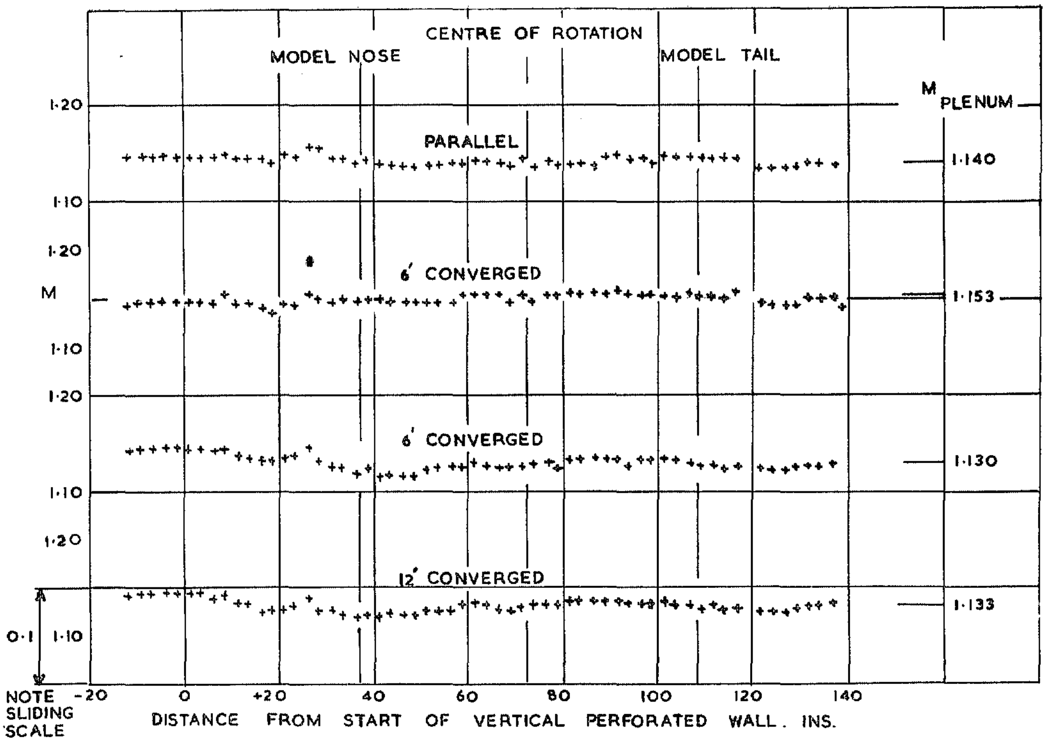

FIG. 21. Effect of perforated-wall convergence on centre-line Mach-number distribution. $M = 1 \cdot 15$ nozzle.

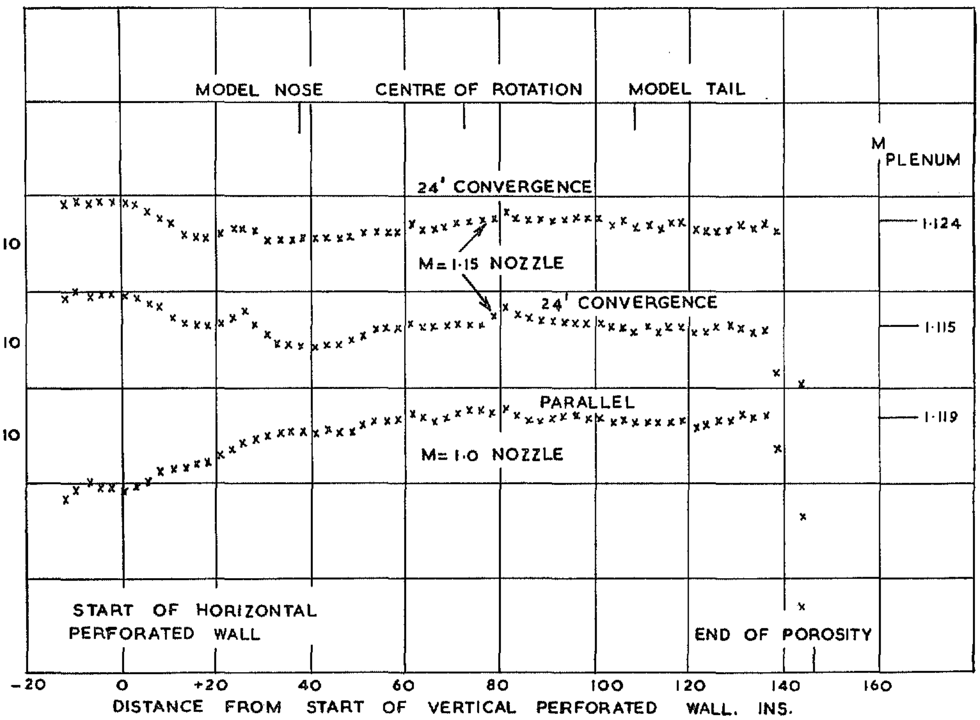

FIG. 22. Comparison of centre-line Mach-number distributions at $M \simeq 1 \cdot 12$ with $M = 1 \cdot 0$ and $M = 1 \cdot 15$ nozzle.

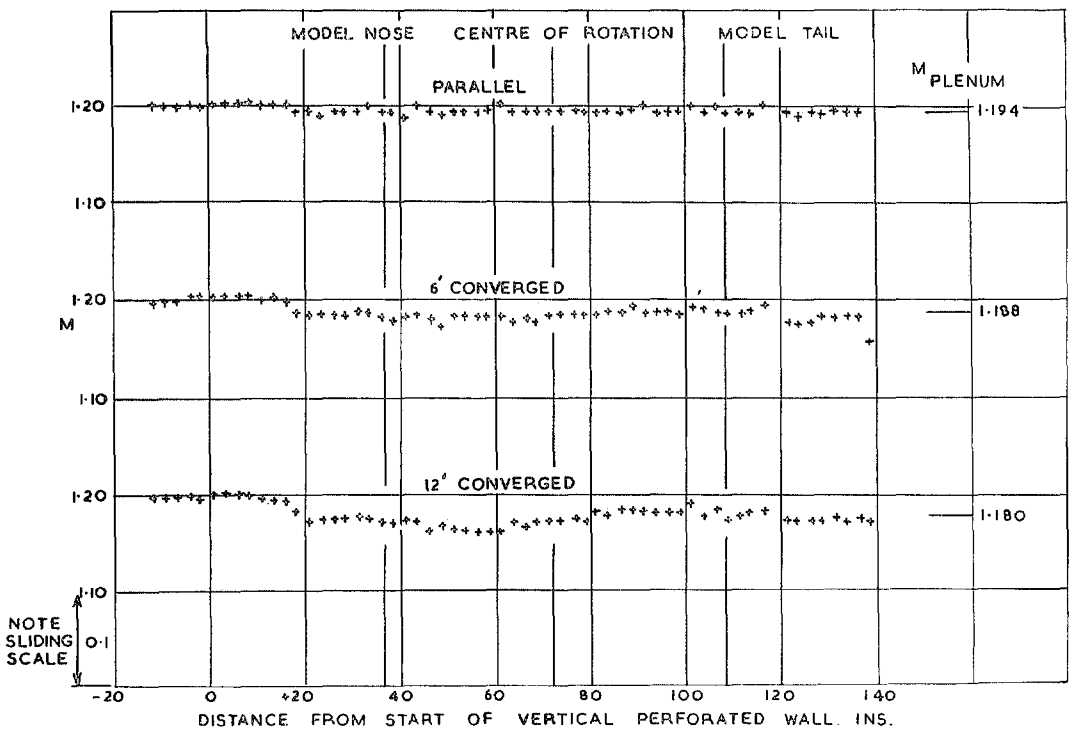

FIG. 23. Effect of perforated-wall convergence on centre-line Mach-number distribution. $M = 1 \cdot 20$ nozzle.

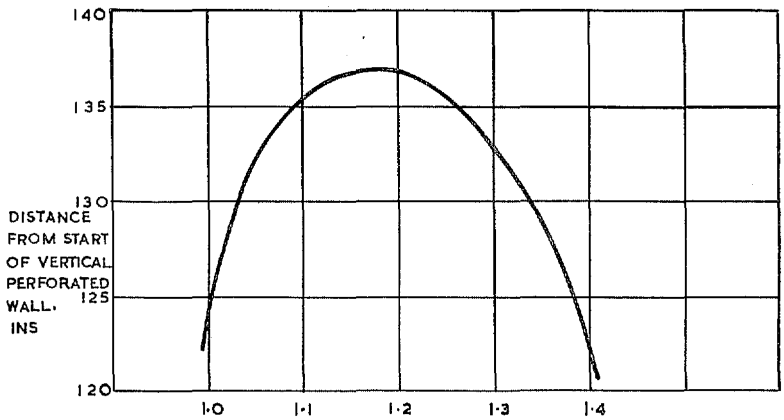

FIG. 24. Variation of fall-off position with plenum Mach number (Perforated walls parallel, $M_{\text{plenum}} = M_{\text{nozzle}}$ fall-off position defined as the point at which the centre-line Mach number is 0·99 plenum Mach number).

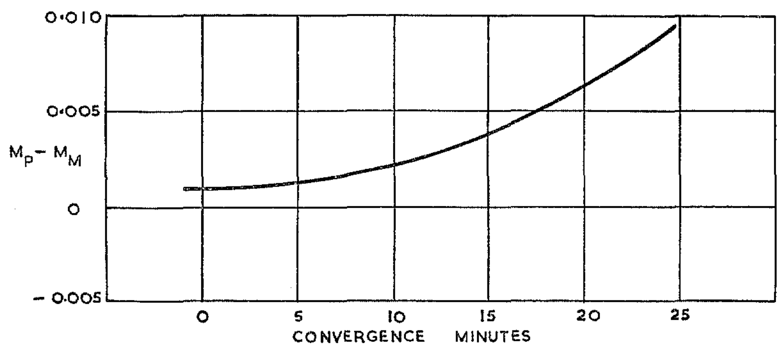

FIG. 25. Effect of perforated-wall convergence on the error in M_{plenum} as an indication of the average centre-line Mach number over the region occupied by a typical model.

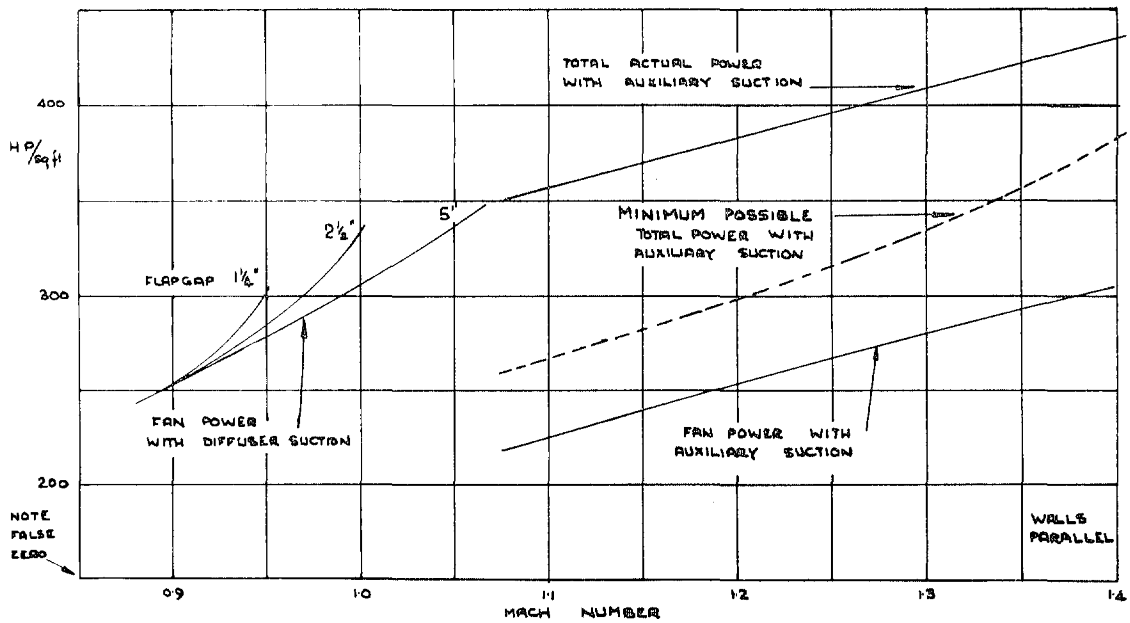

FIG. 26. Tunnel power as motor shaft h.p. per sq ft of working-section at 30 in. Hg stagnation pressure and 40 deg C stagnation temperature.—Tunnel with complete model support but no model.

(78646) Wt. 54/8210 K.5 3/60 Hw.

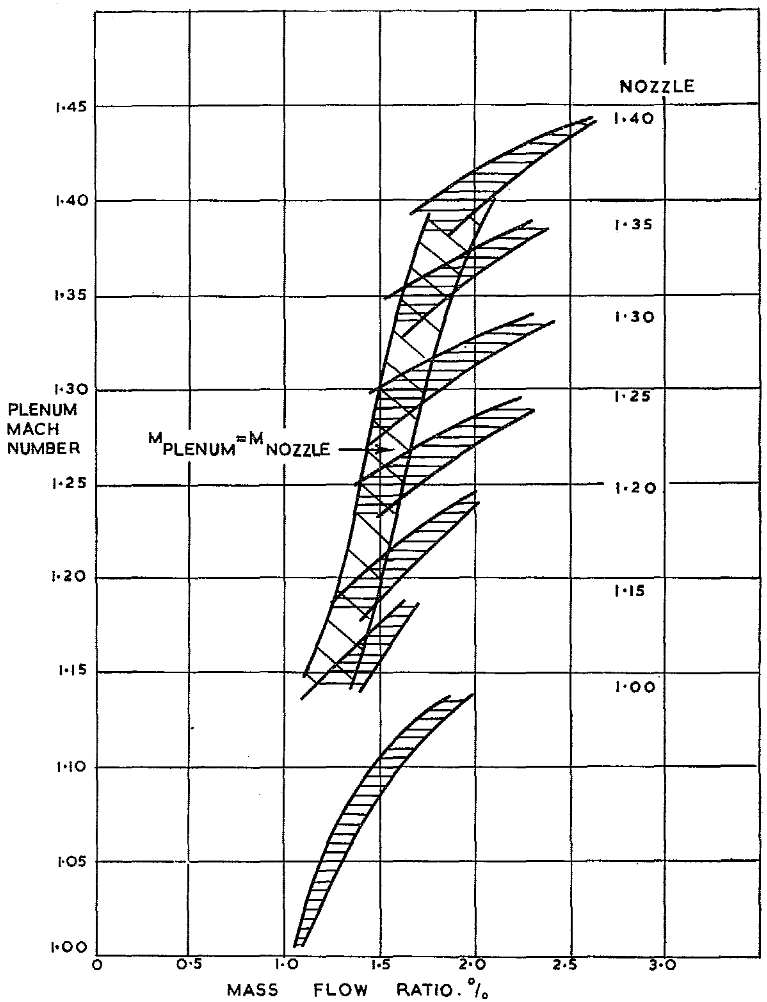

FIG. 27. Variation of auxiliary suction/tunnel mass-flow ratio with plenum Mach numbers.—Perforated walls parallel. Zero diffuser flap gap.

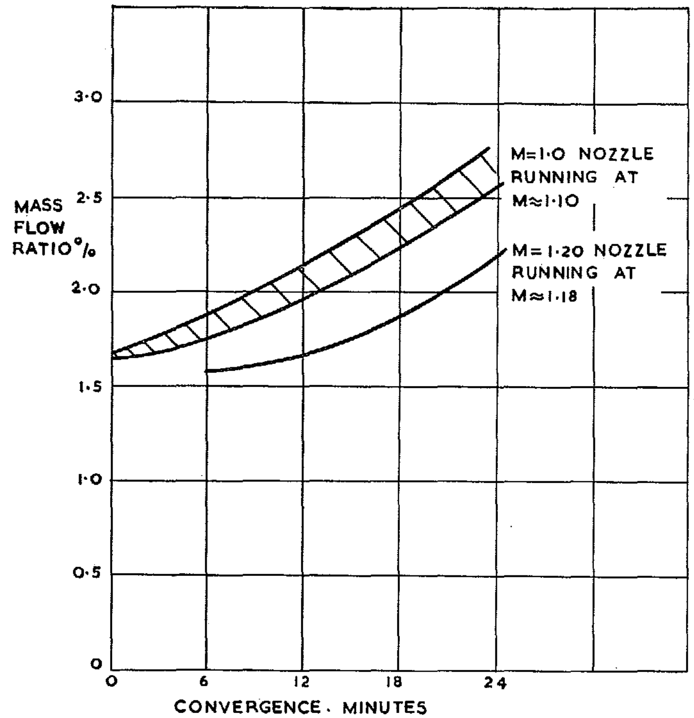

FIG. 28. Effect of perforated-wall convergence on the auxiliary suction/tunnel mass-flow ratio.—$M = 1 \cdot 0$ nozzle running at $M \approx 1 \cdot 10$. $M = 1 \cdot 20$ nozzle running at $M \approx 1 \cdot 18$. Zero diffuser flap gap.

Printed and published by
HER MAJESTY'S STATIONERY OFFICE

To be purchased from
York House, Kingsway, London W.C.2
423 Oxford Street, London W.1
13A Castle Street, Edinburgh 2
109 St. Mary Street, Cardiff
39 King Street, Manchester 2
Tower Lane, Bristol 1
2 Edmund Street, Birmingham 3
80 Chichester Street, Belfast 1
or through any bookseller

Printed in England

R. & M. No. 3140

S.O. Code No. 23-3140